April 2017 version.1

Seasonal phosphorus dynamics in a temperate shelf sea (Celtic Sea): uptake, release, turnover and stoichiometry

Alex J. Poulton[1,2], Clare E. Davis[3], Chris J. Daniels[2], Kyle M.J. Mayers[4], Carolyn Harris[5], Glen A. Tarran[5], Claire E. Widdicombe[5], and E. Malcolm S. Woodward[5]

[1] The Lyell Centre, Heriot-Watt University, Edinburgh, UK

[2] National Oceanography Centre, Waterfront Campus, Southampton, UK

[3] Department of Earth, Ocean and Ecological Sciences, University of Liverpool, Liverpool, UK

[4] Ocean and Earth Science, University of Southampton, National Oceanography Centre Southampton, Southampton, UK

[5] Plymouth Marine Laboratory, Citadel Hill, Plymouth, UK

* Corresponding author.

Tel: +44 7810084597.

Email address: aljp01@gmail.com

Highlights:

- Seasonal phosphorus uptake and dissolved organic release examined in the Central Celtic Sea
- Uptake highest in spring bloom, with biomass-normalised uptake equal in spring and summer
- Release high in November and late spring, with efficient P-retention in summer
- Strong phytoplankton influence on spring P-uptake, whilst bacteria influential in summer
- Relatively C-rich uptake in November and late April, strongly P-rich in summer

Abstract

The seasonal cycle of resource availability in shelf seas has a strong selective pressure on phytoplankton diversity and the biogeochemical cycling of key elements, such as carbon (C) and phosphorus (P). Shifts in carbon consumption relative to P availability, via changes in cellular stoichiometry for example, can lead to an apparent 'excess' of carbon production. We made measurements of inorganic P (P_i) uptake, in parallel to C-fixation, by plankton communities in the Central Celtic Sea (NW European Shelf) in spring (April 2015), summer (July 2015) and fall (November 2014). Short-term (<6 h) P_i-uptake coupled with dissolved organic phosphorus (DOP) release, in parallel to net (24 h) primary production (NPP), were all measured across an irradiance gradient designed to typify vertically and seasonally varying light conditions. Rates of P_i-uptake were highest during spring and lowest in light-limited fall conditions, although biomass-normalised P_i-uptake was similar in spring and summer. The release of DOP was highest in November and declined to low levels in July, indicative of efficient utilization and recycling of the low levels of P_i available. Examination of turnover times of the different particulate pools, including phytoplankton and bacteria, indicated a differing seasonal influence of autotrophs and heterotrophs in P-dynamics, with summer conditions associated with a strong bacterial influence and early spring with fast growing phytoplankton. These seasonal changes in plankton composition, coupled with changes in resource availability (P_i, light) resulted in seasonal changes in the stoichiometry of NPP to P_i-uptake (C:P ratio); from relatively C-rich uptake in November and late April, to P-rich uptake in early April and July. Overall these results highlight how the entire plankton community, both autotrophs and heterotrophs, influence the relative uptake of C and P and that any excess C-consumption relative to the P-rich uptake must be balanced by C-rich process such as the heterotrophic remineralisation and/or consumption of organic material.

Keywords: Phosphorus; Phosphate uptake; Dissolved organic Phosphorus; Stoichiometry.

Regional index terms: Celtic Sea; Northwest European Shelf.

1. Introduction

Phosphorus (P) is an essential nutrient for marine organisms, forming an important component of various cellular constituents, including cell membranes, nucleic acids (RNA, DNA) and in the transmission of chemical energy (Benitez-Nelson, 2000; Karl, 2000; Dyhram et al., 2002). The availability of P is considered to have an important role in controlling planktonic biomass, production and community composition (Karl et al., 2001), with regionally low (pM) P concentrations limiting biomass accumulation and biogeochemical processes (Moore et al., 2013). The biological cycling of nutrients (P, N) are strongly coupled to the carbon (C) cycle via oceanic biomass, resulting in biological processes, such photosynthesis and respiration, having a strong influence on atmospheric CO_2 (Sterner and Elser, 2002; Arrigo, 2005).

The elemental stoichiometry (C:P, C:N) of plankton also propagates through marine food webs to shape ecosystem structure and function (Elser et al., 2000; Sterner and Elser, 2002), and hence plankton provide an interface linking biogeochemical cycles, ecosystem dynamics and global climate (Arrigo, 2005; Finkel et al., 2010). Understanding microbial elemental stoichiometry is important as these relationships play major roles in coupled elemental cycles (Falkowski and Davis, 2004). Planktonic micro-organisms, such as heterotrophic bacteria and phytoplankton, have rapid growth rates and hence can exert a strong influence on the turnover of different C and P pools (Arrigo, 2005). Both phytoplankton and heterotrophic bacteria consume P, though the two have contradictory roles in the marine C-cycle as primary producers and remineralisers of organic material, respectively (Duhamel and Moutin, 2009), and compete strongly for available P (Thingstad et al., 1993, 1996).

Redfield (e.g., Redfield et al., 1963) proposed that plankton and particulate material have a relatively constrained elemental ratio (C:N:P) of 106:16:1, and this matches closely with the average ratio of dissolved inorganic N and P in seawater. These observations led to the paradigm that plankton consume inorganic N and P in the same proportion as they are availability, fixing them into particulate organic material which is eventually decomposed, returning N and P back into their inorganic forms (Redfield et al., 1963). This paradigm of elemental stoichiometry has been used to link plankton production to the biogeochemical cycling of C, N and P. However, it is also recognised that important deviations from the canconical Redfield ratio may occur in the biochemical composition of marine plankton (e.g., Geider and La Roche, 2002; Ho et al., 2003; Finkel et al., 2006), trophic interactions (e.g., Sterner and Elser, 2002; Hessen et al., 2002, 2004) and biogeochemical processes (e.g., Arrigo, 2005; Bozec et al., 2006; Bauer et al., 2013).

As different cellular components, such as proteins and pigments, have their own stoichiometric characteristics and represent significant amounts of the material in plankton cells, changes in their relative proportions strongly influence bulk stoichiometry (Falkowski, 2000; Geider and La Roche, 2002). Under nutrient limited growth conditions plankton show increased cellular quotas of C, suggesting increased uptake and storage of C-rich compounds (e.g., Geider and La Roche, 2002; Hessen et al., 2002, 2008). Rapid growth rates have been predicted to lead to P-rich biomass as the cellular components required for cell division have a high P-content (i.e., 'the growth rate hypothesis'; Elser et al., 2000; Sterner and Elser, 2002). Variability in phytoplankton cellular composition (chlorophyll content, elemental stoichiometry) also influences their quality as food items for higher trophic levels, impacting their growth rates and trophic transfer (e.g., Hessen et al., 2002, 2004, 2008; Sterner and Elser, 2002).

The role of variable elemental stoichiometry is an important component in the C-sequestration efficiency of the Continental Shelf Pump (CSP) (Thomas et al., 2005; Bozec et al., 2006). Seasonal changes in DIC and nutrient drawdown in the North Sea shows that assuming Redfield stoichiometry, C-overconsumption occurs relative to nutrient utilization, with this overconsumption suggested to be supported by changes in plankton stoichiometry under seasonally varying resource (light, nutrient) availability (Toggweiler et al., 1993; Thomas et al., 2005; Bozec et al., 2006; Kuhn et al., 2010). As shelf seas represent less than 10% of the global ocean area, but are responsible for 10 to 30% of primary production and high proportions of global carbon sequestration (Joint et al., 2001; Simpson and Sharples, 2012; Bauer et al., 2013), determining the processes which underpin the magnitude and efficiency of the CSP is an important step. The stoichiometry of primary production, nutrient uptake and recycling, trophic transfer and material decomposition all influence the metabolic balance of shelf seas and the efficiency of the CSP (Bauer et al., 2013).

The aims of the present study were to: (1) explore the seasonal patterns in both P_i-uptake and P-release (DOP production) relative to variability in water-column structure, nutrient (N, P) availability and plankton community composition; and (2) examine the dynamics of P-biogeochemistry in terms of the turnover of different P pools and the stoichiometry of P_i uptake relative to C-fixation (net primary production, NPP). Overall this paper contributes to understanding how the internal biogeochemical cycling of elements contributes to the maintenance and efficiency of the CSP in the Celtic Sea. The specific hypotheses examined are that: (a) the spring bloom uses C and P at close to canconical Redfield ratios due to the optimal growth conditions; (b) whilst departures from the Redfield ratio occur in response to changes in resource availability, such as C-rich production in summer when nutrient levels are depleted.

2. Methods

2.1. Sampling

The present study presents data collected from three cruises onboard the *RRS Discovery* to the Celtic Sea over the period 2014 to 2015; the first in November 2014 (DY018: 9th November to 2nd December), the second in April 2015 (DY029: 1st April to 29th April), and the third and final in July 2015 (DY033: 11th July to 2nd August). Each cruise focused on a different time-period relevant to the ecosystem and biogeochemistry of the Celtic Sea, from the spring bloom (April) to summer stratified period (July), and onto the late autumn bloom and break down of stratification (November). As part of this study, two sites were sampled for phosphate dynamics and ancillary parameters, with the main site in the Central Celtic Sea (CCS; ~49^{o}24' N, 8^{o}36'W; 150 m water depth) and the second at the Shelf Break (CS2; ~48^{o}34.26'W, 9^{o}30.58' W; 203 m water depth) (Fig. 1). Over the three-month sampling period these sites were repeatedly sampled, though CCS was more frequently sampled (n = 15) than CS2 (n = 6).

Water samples were collected from six light depths in 20 L Niskin bottles on a CTD rosette sampler deployed pre-dawn (02:00-06:00 h local time) at CCS and CS2. The light depths sampled were the depths of 60, 40, 20, 10, 5 and 1% of surface irradiance (Photosynthetically Active Radiation, PAR). Pre-dawn sampling depths were determined by back calculation of the vertical attenuation coefficient of PAR (K_d, m^{-1}) based on either (a) an assumption that the base of the surface mixed layer (thermocline) was at or close to the depth of the euphotic zone (i.e. 1% of surface irradiance) (November, April), or (b) that the sub-surface chlorophyll-*a* maximum (SCM) occurred at or close to a depth of 5% of surface irradiance (Hickman et al., 2012) (July).

Surface mixed layer (SML) depths were determined from processed CTD density data (Hopkins, Liverpool, pers. comm.) through a two-step process: firstly, SMLs were identified automatically by applying a threshold for change in potential density with depth (an increase of either 0.02 kg m^{-3} (November, July) or 0.01 kg m^{-3} (April) from the potential density at 10 m (or the nearest available measurement)); and secondly, visual examination and confirmation for profiles that failed these criteria or were close to the thresholds selected. Automatic detection of SML depths was successful at CCS, though there were issues at CS2 due to internal wave breaking and at CCS during April as the stratification of the water-column evolved (Hopkins, Liverpool, pers. comm.). Identification of the thermocline during the cruise was based on unprocessed CTD temperature data, while SML identification was based on processed CTD density data. Hence, differences in SML and euphotic zone depths during November and April are possible due to discrepancies in these data sources and physical complexities of the water-column (especially during April and at the shelf break).

2.2. Incubations

Water samples for NPP, P_i-uptake and DOP production were all incubated in a purposely converted and refitted commercial refrigeration container located on the mezzanine deck of the ship (see Richier et al., 2014) allowing incubation temperatures to be regulated at in situ values (± 1-2^{o}C). Each of the six percentage light depths (60, 40, 20, 10, 5 and 1% of surface irradiance) had a dedicated incubation chamber build, using black-out material to remove any light contamination between the different light chambers. Irradiance was provided by one to three daylight simulation LED panels (Powerpax, UK), each providing up to 100 µmol photons m^{-2} s^{-1}, combined with different types of neutral density filters (Lee Filters^{TM}, UK) to achieve a target irradiance per incubation chamber of 10 to 300 µmol photons m^{-2} s^{-1}. The light-dark cycle was varied between different cruises to accurately represent seasonal variability in photo-period; 9 h in November, 14 h in April and 16 h in July.

To determine the seasonal range in incidental irradiance and allow representative daily light doses to be determined for each light depth and each cruise, weekly average daily PAR levels (mol photons m^2 d^{-1}) over a ten-year period (2003 to 2013) was determined from MODIS Aqua data. Monthly averages over the ten years for incidental irradiance (E_0) for each cruise period were then calculated for the position of the CCS site, giving values of 9.4 mol photons m^{-2} d^{-1} (November), 36.8 mol photons m^{-2} d^{-1} (April), and 43.2 mol photons m^{-2} d^{-1} (July). Actual irradiance levels (E_0) during each cruise were measured by the *RRS Discovery 2π* PAR irradiance sensor (Skye Instruments, SKE 510), with cruise averages (Table 1) showing excellent agreement with long-term monthly averages.

Incidental irradiance for each month were corrected for reflective losses at the sea surface, assuming an 8% loss (D. McKee, Strathclyde, pers. comm.), to give incidental irradiance (100%) values and allow calculation of a light dose for each percentage irradiance chamber. Daily light doses (mol photons m^{-2} d^{-1}) were reconstructed using a combination of one to three daylight simulation LED panels (Powerpax, UK), each providing up to 100 µmol photons m^{-2} s^{-1}, combined with different types of neutral density filters (Lee Filters^{TM}, UK) to achieve a target incidental irradiance per incubation chamber of 7 to 440 µmol photons m^{-2} s^{-1}, which were combined with the appropriate seasonal day length to give a representative seasonal daily light dose for each percentage light depth (See Supplementary Table S1).

In summer when strong vertical stratification occurred across the euphotic zone, the deeper light depth (1%) were incubated in a Fytoscope FS130 laboratory incubator (Photon System Instr., Czech Republic) at in situ temperatures (± 1^{o}C) and with a white LED light panel to replicate the required light dose (See Supplementary Table S1). All light levels in the incubation chambers and Fytoscope were checked with a *4π* scalar PAR irradiance sensor (Biophysical Instruments, QSL-2101).

[Euphotic zone inventories] [Sampling depths] [Incubation irradiances]

2.3. Inorganic Phosphate Uptake and Release of Dissolved Organic Phosphorus

Hourly rates (dawn to midday, ~6-8 h) of inorganic phosphate uptake (P_i-uptake) were determined following Rees et al. (1999), Björkman et al. (2000), and Reynolds et al. (2014). Water samples from the six light depths were collected directly from the CTD under low-light conditions into 0.5 L brown Nalgene™ bottles which were returned to the laboratory for sub-sampling. Under low light conditions, sub-samples (3 light, 1 dark) were then dispensed into 70 mL polycarbonate flasks (Corning, Inc.) and each bottle spiked with either 111-222 kBq ^{33}P-labelled Orthophosphoric acid (PerkinElmer, Inc., specific activity 37 kBq nmol^{-1}) during April 2015 and November 2014 or 333 kBq ^{33}P-labelled Orthophosphoric acid (Hartman Analytical GmbH, specific activity 111 kBq pmol^{-1}) during July 2015. Use of these two isotopes ensured low P_i addition and no enrichment of the ambient P_i pools; in the case of April and November the spike addition resulted in ~3-6 nmol P (<3% of ambient P_i concentrations), and ~9 pmol in July (<1% of ambient P_i concentrations). From one light bottle per light depth, three aliquots of 100 µL was then removed and placed into a 7 mL glass scintillation vial to which 6 mL of Ultima Gold™ (PerkinElmer, Inc.) liquid scintillation cocktail was added and initial activities were counted on a Tri-Carb 3110TR scintillation counter onboard. Triplicate light bottles and the single dark bottle were then incubated in the CT reefer incubators for 6-8 h at six irradiance levels (see previous Section).

To determine P_i-uptake, incubations were terminated by filtration of each sample bottle (3 light, 1 dark) onto a 25 mm diameter 0.45 µm polycarbonate Nuclepore filter under gentle pressure. Filtered samples were rinsed with unlabelled Whatman GF/F filtered seawater, air-dried and placed in a 7 mL glass scintillation vial and 6 mL of Ultima Gold™ (PerkinElmer, Inc.) liquid scintillation cocktail added. Activity on the filters was then determined on a Tri-Carb 3100TR scintillation counter, with P_i-uptake calculated following Björkman et al. (2000).

To determine the release of Dissolved Organic Phosphorus (DOP), at the end the incubation period, 10 mL aliquots were removed from each the four sample bottles (3 light, 1 dark) from three light depths (60, 20 and 1% during November and April, 60, 5 and 1% during July) and gently filtered through 25 mm diameter 0.2 µm Whatman NucleporeTM polycarbonate filters to remove particulate material and the filtrate caught in 15 mL glass test tubes (10% HCl acid-washed, MilliQ rinsed and oven-dried). Each 10 mL aliquot was then transferred to a plastic 15 mL centrifuge tube and 250 µL of a 1 M sodium hydroxide solution (Sigma-Aldrich, UK) added to precipitate out the dissolved P_i and leave the ^{33}P-labelled DOP (Karl and Tien, 1992; Thomson-Bulldis and Karl, 1998; Björkman et al., 2000). Aliquots were shaken vigorously and centrifuged for 1 h at 3500 rpm,

with 1 mL of the supernatant removed from each and placed in a 7 mL glass scintillation vial with 6 mL of Ultima Gold^{TM} (PerkinElmer, Inc.) liquid scintillation cocktail. The activity of the filtrate was then measured in a TriCarb 3100TR scintillation counter.

To estimate the proportion of DOP exuded relative to the phosphate consumed, the gross rate of P_i uptake was estimated as the rate of P_i-uptake plus the rate of DOP production. Hence, we calculated a Percentage Extracellular Release for DOP as the fraction of total DOP uptake (the sum of P_i-uptake and DOP production) represented by DOP production alone, multiplied by 100.

The average RSD (= Standard deviation/Average x 100) of triplicate P_i-uptake measurements was 13% (2-49%) for November, 18% (3-67%) for April and 18% (1-66%) for July. The average RSD of triplicate DOP production measurements was 31% (1-94%) for November, 17% (1-39%) for April and 20% (2-53%) for July.

[Hourly and daily values/integration]

2.5. Particulate Organic Phosphorus and Dissolved Organic Phosphorus

Water samples for determination of the concentrations of Particulate Organic Phosphorus (POP) were collected from 8 depths (Clare?). Water samples (1 L) for POP concentrations were filtered onto 25 mm Whatman GF/F (pre-combusted and HCl acid-washed) glass-fibre filters (effective pore size 0.7 µm) on a plastic filtering rig under less than 12 kPa vacuum pressure. Filters were dried and POP concentrations determined by combustion and acid hydrolysis, with the precision of analysis typically better than 5%.

Sampling and storage bottles for POP and DOP were pre-cleaned with 10% hydrochloric acid and rinsed with MilliQ before use. Samples for DOP were pre-filtered through a combusted and acid-rinsed Whatman GF/F filter and stored in HDPE bottles at -20^{o}C before analysis. DOP concentrations were determined in triplicate by measuring the difference in phosphate concentration before (total phosphate) and after (total dissolved phosphate, TDP) UV oxidation of seawater samples for 2 h. The limits of detection for DOP were 80 nM, and the precision of analysis was typically better than 10%.

2.6. Nutrients and Chlorophyll-a

Water samples for determination of nutrient concentrations (nitrate+nitrite, phosphate, and silicic acid) were collected directly from the CTD into aged, acid washed and MilliQ rinsed 60 mL HDPE Nalgene^{TM} bottles. Nutrient concentrations were determined onboard using a 5-channel Bran and Luebbe AAII segmented flow auto-analyser following the molybdenum blue method (all cruises) or

using a 2 m liquid waveguide capillary cell to check when phosphate concentrations were less than 50 nM. Analytical chemical methodologies used were Brewer and Riley (1965), Grasshoff (1976), Kirkwood (1989) and Mantoura and Woodward (1983).

Water samples (0.2-0.25 L) for chlorophyll-*a* extraction were filtered onto 25 mm diameter Whatman GF/F or Fisherbrand MF300 glass fibre filters (effective pore sizes 0.7 µm) and extracted in 6-10 mL 90% acetone (HPLC grade, Sigma-Aldrich, UK) at -4^{o}C for 18-24 h (Hickman et al., this issue). Fluorescence was measured on a Turner Designs Trilogy fluorometer using a non-acidification module and calibrated with a solid standard and a pure chlorophyll-*a* standard (Sigma-Aldrich, UK).

2.7. Primary Production

Daily rates (dawn to dawn, 24 h) of primary production (i.e. net Primary Production, NPP) included in this paper were determined following the methodology outlined by Mayers et al. (this issue) and Poulton et al. (2014). Briefly, seawater samples were collected from the same six light depths as for Pi-uptake (see Section 2.3) directly from 20 L Niskin bottles on the CTD rosette into 0.5 L brown Nalgene^{TM} bottles (10% HCl acid-washed, MilliQ rinsed) and transferred under low light conditions to the laboratory. In the laboratory, four (3 light, 1 formalin-killed blank) 70 mL polycarbonate (Corning^{TM}) flasks were filled per light depth. Carbon-14 labelled sodium bicarbonate (1258-1628 kBq) was added to each bottle and then three of the bottles were incubated at the relevant light level in the CT Reefer container for 24 h (see Section 2.2). The fourth sample (formalin-blank) had 1 mL of borate buffered formaldehyde added and was incubated alongside the other samples to measure abiotic uptake.

Incubations were terminated by filtering onto 25 mm 0.45 µm Whatman Nuclepore^{TM} polycarbonate filters, with extensive rinsing to remove any unfixed ^{14}C-labelled sodium bicarbonate remaining on the filters. Organic (NPP) carbon fixation was determined using the micro-diffusion technique (see Mayers et al., this issue) in 20 mL glass vials with 1 mL of 1% Orthophosphoric acid added to remove any ^{14}C-particulate inorganic carbon and 10-15 mL of Ultima Gold^{TM} (PerkinElmer, Inc.) liquid scintillation cocktail added to each sample. The activity on the filters was then determined on a Tri-Carb 3100TR liquid scintillation counter onboard. Spike activity was checked by removal of triplicate 100 µL subsamples directly after spike addition and mixing with 200 µL of β-phenylethylamine (Sigma-Aldrich, UK) followed by Ultima Gold^{TM} addition and liquid scintillation counting. The average RSD of triplicate NPP measurements was 15% (2-44%) for November, 14% (1-59%) for April and 11% (1-42%) for July. The formalin blank consistently represented less than 2% of NPP rates (cruise averages: 2%, November; 2%, April; 1%, July).

2.8. Phytoplankton and Bacterial Carbon

Cell abundances for the major phytoplankton groups were analysed from each sampling depth within the euphotic zone, through either flow cytometry (for *Synechococcus*, *Prochlorococcus*, pico-eukaryotes, nano-eukaryotes, coccolithophores, cryptophytes, bacteria) or light microscopy (for diatoms and autotrophic dinoflagellates). Samples for flow cytometry were collected in clean 250 mL polycarbonate bottles and analysed using a Becton Dickinson FACSort instrument while samples for light microscopy were collected in 100 mL brown glass bottles and preserved in acidic Lugol's solution (2% final solution) until analysis under a Leica DM IRB inverted microscope (Widdicombe et al., 2010).

Cell abundances from flow cytometer counts were converted to biomass using literature values (Tarran et al., 2006): specifically, 8.58 fmol C $cell^{-1}$ for *Synechococcus*, 2.67 fmol C $cell^{-1}$ for *Prochlorococcus*, 36.67 fmol C $cell^{-1}$ for picoeukaryotes, 0.76 pmol C $cell^{-1}$ for nano-eukaryotes, 1.08 pmol C $cell^{-1}$ for coccolithophores, and 1.97 pmol C $cell^{-1}$ for cryptophytes. Heterotrophic bacteria counts were converted to biomass using values of 1.58 fmol C $cell^{-1}$ for 'High Nucleic Acid' and 0.91 fmol C $cell^{-1}$ for 'Low Nucleic Acid' containing cells. Cellular biomass for light microscope counted taxa (diatoms and autotrophic dinoflagellates) were estimated from cell dimensions following Kovala and Larrence (1966) on an individual species basis. For the estimates of phytoplankton carbon used in this study, a geometric mean value for all species present in the samples was used: specifically, 19.58 pmol C $cell^{-1}$ for diatoms and 85.25 pmol C $cell^{-1}$ for autotrophic dinoflagellates.

3. Results

3.1. Seasonal changes in environmental conditions in the Celtic Sea

Clear seasonal variability (Table 1) at both study sites (CCS, CS2) was evident in terms of changes in the depth and average temperature of the surface mixed layer (SML), as well as the surface concentration of inorganic phosphate (P_i) and nitrate+nitrite (NO_x). The SML shallowed from ~50 m to ~20 to 30 m and warmed by ~6^oC between April and July, while it was at its deepest (average 50 m) and at intermediate temperature (12.8-13.9^oC) in November (Table 1). Nutrient concentrations (both P_i and NOx) were highest in early April and declined into low-nutrient (P_i <100 nmol P L^{-1}; NO_x <0.02 µmol N L^{-1}) summer conditions in July (Table 1). Significant temporal variability was also observed throughout April, with the SML shallowing (from 51 to 16 m) and warming by ~1^oC, accompanied by the drawdown of both P_i (~300 nmol P L^{-1}) and NO_x (5.5 µmol N L^{-1}). The ratio of NO_x to P_i, expressed as N* (e.g. Moore et al., 2009), showed that shelf waters were almost always depleted (relative to Redfield) in terms of NO_x, with most N* values well

below zero across all three sampling periods (Table 1). In fact, the N* values per cruise were very similar, with little seasonal variability, whereas the N:P ratio (mol:mol) was high in November and April (~8-12 and 3-12, respectively) and extremely low (<0.5) in July (data not shown).

[Incidental irradiance] [SML average irradiance] [Euphotic zones]

Discrete measurements of P_i over the euphotic zone also showed clear seasonal variability between the sampling periods (Fig. 2a), with vertical differences absent in November and April but clearly present in July. Concentrations of P_i were highest in April (up to 500 nmol P L^{-1}), varying from ~200 to 500 nmol P L^{-1} over the month, and lowest (<100 nmol P L^{-1}) in July, apart from at the base of euphotic zone (>100-600 nmol P L^{-1}) in association with a nutricline (Fig. 2a) and a Sub-surface Chl-*a* Maximum (SCM; Fig. 2b). Euphotic zone Chl-*a* concentrations were also uniform with sampling depth in November and April, while a SCM was evident in July with deep Chl-*a* concentrations ranging from ~0.5 to 2.25 mg m^{-3} (Fig. 2b). The highest Chl-*a* concentrations, and greatest variability, was observed in April during the spring bloom, with Chl-*a* at depth ranging from 1 to 8 mg m^{-3} (Fig. 2b). A slight discrepancy to this pattern in April was observed at the deepest sampling depth where Chl-*a* concentrations were consistently low (1 to 2 mg m^{-3}) and similar to concentrations at depth in November (Fig. 2b).

In terms of DOP concentrations (Fig. 2c), average discrete depth measurements in the euphotic zone were high and relatively similar in November (266 to 389 nmol P L^{-1}) and April (241 to 438 nmol P L^{-1}), and slightly lower in July (169 to 271 nmol P L^{-1}). No distinct depth pattern was evident in either of November, April or July, with upper euphotic zone measurements similar to those found at the base of the euphotic zone. In contrast to DOP, POP concentrations showed a different temporal pattern, with the highest (> 75 nmol P L^{-1}) concentrations in April rather than November or July (<75 nmol P L^{-1}), though this trend was most clearly seen in the upper sampling depths of the euphotic zone (Fig. 2d). Average POP concentrations in April in the upper euphotic zone ranged from 91 to 133 nmol P L^{-1}, with averages in November and July ranging from 28 to 46 nmol P L^{-1} and 23 to 51 nmol P L^{-1}, respectively.

3.2. Vertical profiles of Phosphate uptake

Discrete measurements of P_i-uptake over the euphotic zone (Fig. 3a) also showed clear seasonal differences, with rates in April (>1 nmol P L^{-1} d^{-1}) much higher than those in July (<1.5 nmol P L^{-1} d^{-1}) or November (<0.4 nmol P L^{-1} d^{-1}). Upper euphotic zone P_i-uptake rates ranged from 1.2 to 5.1 nmol P L^{-1} h^{-1} in April, from 0.5 to 2.1 nmol P L^{-1} h^{-1} in July and 0.2 to 0.4 nmol P L^{-1} h^{-1} in November. Uptake of P_i across the incubation light gradients showed light-dependent variability in both November and April, being highest at the higher irradiance levels and decreasing with

declining irradiance (Fig. 3a). In contrast, P_i-uptake in July showed no dependency on incubation irradiance despite the absolute irradiance levels being identical to April, most likely due to limiting P_i concentrations in July (Fig. 2a) and hence substrate rather than irradiance dependency.

The ratio of light P_i-uptake to dark P_i-uptake was most often greater than 1, especially at the irradiance levels greater than ~0.4 mol quanta m^{-2} h^{-1} during all three sampling periods (Fig. 3b). Ratios of light to dark P_i-uptake were only less than 1 at the very lowest irradiance levels (<0.1 mol quanta m^{-2} h^{-1}) in November and April, whereas ratios rarely fell below 1 (or 1.5) during July. Ratios near unity for light to dark Pi-uptake highlight how there was very little difference between light and dark Pi-uptake rates in November and April, whereas a difference was more noticeable in July (Fig. 3b). For example, overall there was a 24% difference in average light and dark P_i-uptake rates in November (0.21 and 0.16 nmol P L^{-1} h^{-1}, respectively), and a 40% difference in July (0.89 and 0.53 nmol P L^{-1} h^{-1}, respectively).

Normalizing the P_i-uptake rates to Chl-*a* concentration gives some measure of P_i-uptake per unit of phytoplankton biomass. Across the three sampling periods, Chl-*a* normalised P_i-uptake was lowest (<0.4 nmol P (µg Chl)$^{-1}$ h^{-1}) in November and reached some of the highest values in July (>2 nmol P (µg Chl)$^{-1}$ h^{-1}), though values were also high during April (Fig. 3c). Biomass-normalised P_i-uptake showed light-dependent variability in both November and July, being highest at the higher irradiances and declining with depth, whereas no variability was evident in April. In July, light-dependency in Chl-*a* normalised P_i-uptake was observed at the higher irradiances (>0.43 mol quanta m^{-2} h^{-1}), whereas biomass-dependency occurred as Chl-*a* normalised rates increased again at the lower irradiances in association with the SCM (see Fig. 2b). In November, the high rates of Chl-*a* normalised P_i-uptake at higher irradiances (Fig. 3c), declining with declining irradiance, is driven by the light-dependency of P_i-uptake (Fig. 3a) as the Chl-*a* profiles were more uniform across sampling depths (Fig. 2b).

3.3. Vertical profiles of DOP production

The short-term production of DOP also showed clear season differences, with rates being low (<0.2 nmol P L^{-1} h^{-1}) in both November and July and high (and more variable) in April (often >0.5 nmol P L^{-1} h^{-1}) (Fig. 4a). Production of DOP over the three sampling depths ranges from 0.07 to 0.39 nmol P L^{-1} h^{-1} in November, from 0.10 to 1.78 nmol P L^{-1} h^{-1} in April and from 0.02 to 0.24 nmol P L^{-1} h^{-1} in July. Hence, although DOP production was similar in November and July, it was slightly lower in July than November, and in April it varied from levels seen in the other months to values 5 to 7 times higher. In all three sampling periods, no variability in DOP production occurred in association with changes in the incubation irradiances (Fig. 4a): light-availability had no obvious influence on

DOP production. Ratios of light to dark DOP production were mostly greater than 1 during all three sampling periods, with very few measurements showing ratios less than 1 (Fig. 4b). Light to dark DOP production ratios also showed no obvious variability in association with incubation irradiance.

Normalising DOP production to Chl-*a* concentrations showed the lowest biomass-normalised rates in November (<0.3 nmol P (µg Chl)$^{-1}$ h^{-1}), with similar low rates in both April and July at the higher incubation irradiances (>0.43 mol quanta m^{-2} h^{-1}) (Fig. 4c). This is contrasted by the pattern at the lowest incubation irradiance (0.03 mol quanta m^{-2} h^{-1}), which during both April and July showed high (>0.3 nmol P (µg Chl)$^{-1}$ h^{-1}) Chl-*a* normalised rates of DOP production. In April, these Chl-*a* normalised rates of DOP production reached as high as 1.46 nmol P (µg Chl)$^{-1}$ h^{-1}, being around half as high in July. In April, these high rates of Chl-*a* normalised DOP production at low irradiance were associated with relatively low Chl-*a* concentrations and high DOP production rates (Figs. 2b and 3a). In July, the high Chl-*a* normalised rates were associated with low DOP production, high P_i concentrations and the SCM (Figs. 2a and 2b). Hence, high Chl-*a* normalised rates in April are linked to high DOP production whereas high rates in July are associated with relatively high levels of biomass (Chl-*a*) and substrate (P_i) availability.

Expressing DOP production as a fraction of total P_i-uptake (i.e. the sum of P_i-uptake and DOP production) shows clear patterns with sampling period and incubation irradiance (Fig. 4d). In November, the percentage extracellular release of DOP is consistently greater than 25% and increases up to 73% with decreasing incubation irradiance. A similar pattern is seen in April, although the levels of DOP release are slightly lower (down to 5-10% in some cases) (Fig. 4d). In contrast, DOP release in July is much lower (<20%) at all incubation irradiances, and in some cases DOP release in July is less than 5% of total Pi-uptake. Clearly, when P_i concentrations are at their lowest in July (<100 nmol P L^{-1}; Fig. 2a), DOP production and extracellular release (Figs. 4a and 4d) are at their lowest level, despite relatively high rates of P_i-uptake (Fig. 3a).

3.4. Integrated euphotic zone inventories

Nutrient concentrations and rates of P cycling were integrated across the euphotic layer for all 3 cruises (November, April and July), which we considered to roughly match the SML in November and early April, and then contain both the SML and thermocline (and SCM) in late April and July (see Table 1).

Euphotic zone integrals of Chl-*a* showed a clear seasonal progression of the phytoplankton communities, with average Chl-*a* concentrations highest in April (37.8-152.6 mg m^{-2}), intermediate in November (37.4-70.8 mg m^{-2}) and lowest in July (17.2-35.7 mg m^{-2}). Within April, Chl-*a* concentrations went from 49.6 mg m^{-2} in early April to a peak value of 152.6 mg m^{-2} in mid-April,

which then decreased again towards the end of the month (Table 2). The mid-April Chl-*a* peak was associated with the spring bloom at the CCS site (Mayers et al., this issue) and discrete water-column Chl-*a* concentrations were as high as 8 mg m^{-3} (Fig. 2b). Increasing Chl-*a* concentrations throughout April were associated with a significant drawdown of P_i, as shown by declining P_i integrals from a high of 18.3 mmol P m^{-2} to values similar to those observed in November and July (i.e. <10 mmol P m^{-2}; Table 2). However, the depth distribution of P_i was drastically different between these two months (Fig. 2a): in November, moderate P_i concentrations (175-225 nmol P L^{-1}) occurred throughout the water-column, while in July P_i concentrations were extremely low (<100 nmol P L^{-1}) in the upper water-column and increased dramatically (up to 600 nmol P L^{-1}) in association with the nutricline. Despite the presence of a SCM in July (Fig. 2b), this month had the lowest water-column inventories for Chl-*a* (Table 2).

[Estimates of integrated phytoplankton biomass (C_{phyto}) (Table 2) and C:Chl ratios; Cbact]

Integrated net primary production (NPP) mirrored the seasonal changes in Chl-*a* concentrations, with rates low in November (average 32.4 mmol C m^{-2} d^{-1}) and July (average 35.4 mmol C m^{-2} d^{-1}) and peaking in mid-April at ~0.5 mol C m^{-2} d^{-1} (Table 2). As with Chl-*a*, April showed relatively low rates of NPP (<120 mmol C m^{-2} d^{-1}) early in the month, a peak on the 15th April and a decline to values roughly half of the peak (132-321 mmol C m^{-2} d^{-1}) at the end of the month. Clearly the spring bloom in 2015 at CCS was associated with significant carbon fixation (see also Mayers et al., this issue). Normalising NPP to Chl-*a* concentrations shows a similar seasonal pattern in terms of the NPP per unit of phytoplankton biomass, with (integrated) Chl-*a* normalised NPP rates similar in November (average 0.7 gC (g Chl)$^{-1}$ h^{-1}) and July (average 1.1 gC (g Chl)$^{-1}$ h^{-1}) and peaking in mid-April with maximum values of 3.0 gC (g Chl)$^{-1}$ h^{-1} (average 2.0 gC (g Chl)$^{-1}$ h^{-1}) (Table 2). Such Chl-*a* normalised NPP rates indicate that phytoplankton communities in November and July were fixing (photosynthetically) around the same amount of C per gram of (Chl-*a*) biomass, while the community in April fixed almost double the amount for the same level of (Chl-*a*) biomass.

Euphotic zone integrals of POP showed a similar April peak to Chl-*a* and NPP, with the highest values in April (range 1.0 to 3.5 mmol P m^{-2}, average 2.3 mmol P m^{-2}), with lower and similar values in July (1.0-2.0 mmol P m^{-2}) and November (1.0-2.2 mmol P m^{-2}) (Table 2). Some of the highest integrated POP values (>3 mmol P m^{-2}) occurred in association with the high levels of Chl-*a* and NPP in mid-April at CCS. In contrast to POP (Chl-*a* and NPP), water-column integrated DOP concentrations showed a different seasonal pattern with integrals in November and April the highest (averages 16 and 11 mmol P m^{-2}, respectively), with lower values (3-10 mmol P m^{-2}) in July (Table 2). In both April and July, integrated DOP concentrations were roughly equivalent to the size of the ambient P_i pool in the euphotic zone, while in November DOP concentrations were higher than P_i.

Though significant P_i drawdown was seen during April, there was no concurrent increase in the DOP pool which only varied in size by ~6-7 mmol P m^{-2} relative to a P_i drawdown of ~12 mmol P m^{-2} and a ~2-3 mmol P m^{-2} increase in POP (Table 2).

The seasonal pattern of euphotic zone integrated P_i-uptake showed a peak in April (average 1.61 mmol P m^{-2} d^{-1}), with the July average roughly half of that in April (0.84 mmol P m^{-2} d^{-1}) and the lowest rates (<0.30 mmol P m-2 d-1) in November (Table 2). The highest rate of integrated P_i-uptake occurred in mid-April (2.08 mmol P m^{-2} d^{-1}) in association with the peak values of Chl-*a* and NPP, although unlike Chl-*a* and NPP, the P_i-uptake rates throughout April were much higher (generally >1.3 mmol P m^{-2} d^{-1}) than those measured during the other sampling periods (range 0.14-0.30 mmol P m^{-2} d^{-1} for November and 0.48-1.18 mmol P m^{-2} d^{-1} for July). In the case of integrated DOP production (Table 2), the highest values occurred in April (average 0.49 mmol P m^{-2} d^{-1}), with values in November ~3 times higher (average 0.17 mmol P m^{-2} d^{-1}) than those in July (average 0.05 mmol P m^{-2} d^{-1}). This pattern contrasts to that of the integrated P_i-uptake, with the highest DOP production (>0.8 mmol P m^{-2} d^{-1}) occurring not in association with the peak in P_i-uptake, Chl-*a* or NPP but rather 5 to 9 days later in April (Table 2). When integrated DOP production is expressed as a fraction of total P_i-uptake (see Section 3.3) there are strong differences between the three sampling periods (Table 2); DOP production represents (on average) a much higher fraction of total P_i-uptake in November (41%) than in April (21%) or July (6%) (Table 2). The percentage extracellular release of DOP is extremely low (<5%) in some cases in early July, with the low values (<15%) seen in July only seen elsewhere during early April, well before the development of the spring bloom and peak Chl-*a* around the 15th April.

Normalising integrated P_i-uptake to integrated Chl-*a* concentrations showed the lowest biomass-normalised rates in November (3.5-5.5 nmol P (µg Chl)$^{-1}$ d^{-1}), with rates similar in April (13.6-43.4 nmol P (µg Chl)$^{-1}$ d^{-1}) and July (17.1-57.5 nmol P (µg Chl)$^{-1}$ d^{-1}) though the averages are slightly different (Table 2). Chl-*a* normalised P_i-uptake showed no clear relationship to the peak in absolute P_i-uptake (Chl-*a* or NPP) in mid-April and the highest Chl-*a* normalised P_i-uptake (57.5 nmol P (µg Chl)$^{-1}$ d^{-1}) occurred in July rather than April. In the case of Chl-*a* normalised DOP production, although April had some of the highest rates (>6 nmol P (µg Chl)$^{-1}$ d^{-1}), in general the Chl-*a* normalised DOP production were similar (~2-5 nmol P (µg Chl)$^{-1}$ d^{-1}) throughout the three sampling periods (Table 2). The highest Chl-*a* normalised DOP production also showed no clear relationship to changes in absolute DOP production (Chl-*a* or NPP), although the highest rate in Chl-*a* normalised DOP production occurred at the same time as the highest DOP production rate, 9 days after the peak in Chl-*a* in April.

4. Discussion

4.1. The dynamics of Phosphate uptake

The uptake of nutrients (N, P) and photosynthetic C-fixation, and the resulting stoichiometric balance of cellular constituents vary on timescales from almost instantaneous to daily adjustments (e.g., Geider and La Roche, 2002; Rees et al., 1999; Talmy et al., 2014; Lopez et al., 2016). Ecological interactions also occur across various timescales, resulting in stoichiometric balances that vary in time and space, with important implications for the biogeochemistry of marine ecosystems (Sterner and Elser, 2002). Short-term measurements need to be scaled to appropriate integral time- and depth-scales (e.g. daily, euphotic zone), and clear perspectives on what is (or is not) measured is required prior to examining system-scale biogeochemical processes.

The potentially rapid recycling of P leads to the requirement that uptake (and release) measurements are considered over short-time periods, whereas photosynthetic C-fixation occurs throughout the (seasonally variable) daylight period. Short-term Pi-uptake measurements are often scaled to a 24 h period, with the inherent assumption that uptake rates are temporally invariable. To examine this, we undertook two time-series incubations of P_i-uptake, with measurements every 4 h over a period of 24 h (Fig. 5). One time-series incubation began at 6 am (local time) on the 17th July and the second at 9 am (local time) on the 23rd July, with both experiments showing a steady increase in P_i-uptake prior to sunset and then a slight decline during the night (Fig. 5a). Average P_i-uptake (± S.D.) for these incubations was 0.72 ± 0.20 and 0.92 ± 0.22 nmol P L^{-1} h^{-1}, respectively, which are higher than the initial 4 h measurements (0.43 ± 0.06 and 0.67 ± 0.08 nmol P L^{-1} h^{-1}, respectively). If the initial measurements are scaled by 24 h daily rates of 9.6 nmol P L^{-1} d^{-1} and 16.8 nmol P L^{-1} d^{-1} are calculated, which are 30 to 40% less than the cumulative 24 h rates (Fig. 5b). These results highlight that short-term rates of P_i-uptake do vary during day- and night-time periods and scaling initial rates may result in a moderate underestimation of daily P_i-uptake.

Across all three seasonal sampling periods, rates of both P_i-uptake and DOP production in light-exposed (L) incubations were higher than those incubated in the dark (D), with L:D ratios consistently greater than 1 (Figs. 3b and 4b). For P_i-uptake, L:D ratios were greater than 1.5 at the highest incubation irradiances (>0.6 mol quanta m^{-2} h^{-1}) in November and April, and across most of the light gradient in July. Light availability clearly enhanced P_i-uptake, which may be analogous to the reduced rates of P_i-uptake during the night-time time-series experiments (Fig. 5a). In the case of DOP production, L:D ratios were also slightly higher than 1 during July, and in general the L:D ratios were similar in magnitude and trend to those seen in P_i-uptake (Fig. 4b): hence the irradiance-influence on P_i-uptake was mirrored in the subsequent release of DOP, though the relative PER of

DOP differed seasonally (Fig. 4d). Ratios of L:D P_i-uptake in other studies have also been found to be greater than 1, for example in the North Atlantic (Donald et al., 2001) and Pacific Ocean (Duhamel et al., 2012), although ratios closer to 1 have been reported from the North Pacific subtropical gyre (Björkman et al. 2000). Variability in L:D uptake ratios likely reflects seasonal variability in substrate (P_i) availability and energetic (light, C) constraints on P_i-uptake and cellular P-demands (Sterner and Elser, 2002; Björkman et al., 2000).

Competition between bacteria and phytoplankton for P is a strong driver of biogeochemistry in marine ecosystems (Thingstad et al., 1993, 1996; Popendorf and Duhamel, 2015). Previous studies of planktonic P_i-uptake have differentiated bacterial and algal P-uptake using different pore-sized filters, for example considering bacterial uptake as from cells less than 0.6 µm and algal uptake from cells greater than 0.6 µm (e.g., Duhamel and Moutin, 2009). However, both bacterial and algal cell sizes are variable with taxonomy and physiological status (ref) and may overlap in size-distribution; for example, the cyanobacteria *Synechococcus*, which is dominant in the Celtic Sea in summer (Hickman et al., 2012), may range in size from 0.4 to 0.8 µm (ref). In this study, 0.45 µm filters were used to ensure that P_i-uptake from *Synechococcus* was fully included in our measurements at the same time as (partly) excluding heterotrophic bacteria.

To test this assumption, size-fractionation experiments were performed with samples size-fractionated (0.2, 0.45, 0.8 and 2 µm) post-incubation to determine the P_i-uptake by different fractions (Supplementary Fig. S1). These experiments indicated that the 0.45 µm P_i-uptake represented 30 to 80% of the total (0.2 µm) P_i-uptake, while the 0.2 to 0.45 µm fraction was responsible for 20 to 70%, the greater than 0.8 µm fraction for 20 to 50%, and the greater than 2 µm fraction 10 to 20%. These differential contributions are similar to those found by Duhamel and Moutin (2009) (~15-43% 0.2-0.6 µm, ~20-75% 0.6-2 µm, ~10-50% >2 µm), implying that although the use of 0.45 µm filters removed a proportion of bacterial P_i-uptake, our measurements of P_i-uptake are not exclusively from phytoplankton and likely include some bacterial P_i-uptake. Hence, when considering the P-dynamics observed seasonally the composition of the plankton community in terms of both phytoplankton and bacteria needs to be considered.

4.2. Seasonal changes in Phosphate uptake and DOP release in the Celtic Sea

Observations from November to July in the Celtic Sea showed clear seasonal patterns in plankton community composition (Hickman et al., this issue; Mayers et al., this issue) and biogeochemical processes (Garcia-Martin et al., this issue-A & B). Phytoplankton biomass (Chl-*a* and C_{phyto}) and NPP both peaked in April and diverged in November and July, with Chl-*a* levels halved in July relative to November although levels of C_{phyto} and NPP were more similar (Tables 1 and 2). This

divergence is linked to seasonality in C to Chl-*a* ratios at CCS, with euphotic zone integral estimated ratios (g:g) varying from an average of 15 in November to 27 in April and 60 in July (ranges: 12-18, 14-37 and 29-124, respectively) (data not shown). These values are similar to estimates by Holligan et al. (1984) for summer in the Celtic Sea, and are driven by cellular responses to seasonal variability in resource (light, nutrients) availability (Geider, 1987; Artega et al., 2016).

Seasonality in C:Chl-*a* ratios at CCS link to variability in P_i (and NO_x) concentrations and $\bar{E}_{SML}$ (Tables 1 and 2); with low $\bar{E}_{SML}$ and high P_i in November and high $\bar{E}_{SML}$ and low P_i in July, whereas April represents a transitional month between these two scenarios. Phytoplankton dynamics at CCS in November may be considered light-driven while July is nutrient-driven, and April transitions from a light- to nutrient-driven scenario. Nitrogen (N) availability has been previously proposed to limit primary production in the Celtic Sea (Pemberton et al., 2004; Davis et al., 2014). Low N* values seen at CCS support this conclusion, along with the depletion of NO_x below detection levels (<20 nM) in July whilst P_i remains above 55 nM (Table 1). The absence of depletion of P_i to 'undetectable levels' (<30 nM; Karl, 2000) in surface waters in summer contrasts with the open-ocean where P_i may be depleted to a few nano-moles and strongly limits NPP (e.g., Krom et al., 1991; Björkman et al., 2000).

As well as phytoplankton biomass (Chl-*a*, C_{phyto}) and NPP, POP also peaked in April (average: 2.3 mmol P m^{-2}) whilst concentrations in November and July were relatively similar (1.4 and 1.5 mmol P m^{-2}, respectively) (Table 2). Although cruise averages for DOP concentrations appear high in November, declining to low values in July, the range of values per sampling period do show similar values (ranges: 11-25, 6-13, 3-10 mmol P m^{-2}). Lower DOP concentrations in July could be associated with the bacterial utilization of DOP, via hydrolytic enzymes such as alkaline phosphatase, which occurs in severely P-stressed conditions (Dyhram and Ruttenberg, 2006; Dyhram et al., 2007; Duhamel et al., 2013). Summation of the different P pools (P_i, POP and DOP) at CCS shows only a slight decline in the total P pool (averages: 29.4 to 24.2 mmol P m^{-2} from November to April, down to 12.2 mmol P m^{-2} in July), with the proportion of total P in the DOP and P_i pools remaining ~45 to 56% and 34 to 39%, respectively, and the fraction in the POP pool increases slightly from ~5% in November to 14% in July (data not shown). Hence, there is a loss of P from the euphotic zone which may be linked to sinking of material below the thermocline and/or the advection of semi-labile DOP (Reynolds et al., 2014).

April was also associated with a peak in P_i-uptake, with rates in July four times higher than those in November, despite the significantly reduced nutrient concentrations and sizes of the nutrient pools (Tables 1 and 2). Biomass (Chl-*a*) normalised rates of P_i-uptake were in fact highest in July rather

than April (cruise averages: 35.4 and 22.5 nmol P (µg Chl-*a*)$^{-1}$ d^{-1}), and almost an order of magnitude lower in November (Table 2). This implies that P_i-uptake per unit of autotrophic biomass was most efficient in July, however if the seasonal change in C:Chl-*a* ratios are also considered then average C_{phyto} normalised rates of P_i-uptake are much more similar between April and July (both ~9.4 nmol P (mmol C)$^{-1}$ d^{-1}) than November (3.2 nmol P (mmol C)$^{-1}$ d^{-1}). These C_{phyto} normalised P_i rates indicate that the affinity of P_i-uptake was highest, and of equal magnitude, in spring (April) and summer (July) in the Celtic Sea.

An alternative expression of the affinity of Pi-uptake is a biomass-specific turnover rate ($1/P_i$ turnover x POP), where the biomass is represented by POP and the units are proportional to the volume of water cleared of substrate per unit biomass per unit time (Thingstad and Rassoulzadegan, 1999; Tambi et al., 2009). For CCS, average values for November were 1.1 L pmol P^{-1} h^{-1} and were then 5-times higher in April (5.4 L pmol P^{-1} h^{-1}) and 10-times higher in July (11.1 L pmol P^{-1} h^{-1}); indicating that the affinity for P_i-uptake was highest in summer rather than spring. The amount of this P_i taken up by the plankton that is then released as DOP also varies between April and July, with the PER of DOP highest in November (31-58%), and then roughly halving into April (7-45%) and July (2-11%) (Table 2). The summertime planktonic ecosystem at CCS was highly efficient (high affinity) at P_i-uptake and P-retention in organic particles, whilst there was a 'loss' of P from the dissolved inorganic and organic pools. In contrast, the November ecosystem at CCS was least efficient (low affinity) at P_i-uptake or P-retention, with light (low $\bar{E}_{SML}$) as the most likely limiting factor for this community (Table 1).

4.3. Seasonal changes in the turnover of the different P pools in the Celtic Sea

Consideration of only the pool sizes or discrete concentrations and uptake rates gives limited insights into biogeochemical processes. Rather, consideration of the turnover rates of the different pools accounts for both the relative pool size and the uptake rate, providing further information on the dynamics of the system (Benitez-Nelson, 2000). Short (fast) turnover times (a few hrs or days) implies rapid biological utilization or significant demand, whilst longer (slower) turnover times (>1 week or longer) indicate a lack of bioavailability or lower requirements (Benitez-Nelson, 2000). Comparison of turnover times of related pools (e.g., C_{phyto} and POC; Poulton et al., 2006) also provides further insights into underlying ecological and biogeochemical processes.

Phytoplankton turnover times at CCS, calculated from C_{phyto} and NPP (following Leynaert et al., 2000; see also Poulton et al., 2006), shows strong seasonality with short turnover times (<1 day) in April compared with longer turnover times in both November and July (1.5-2.2 d and 1.1-4.4 d, respectively) (Table 3). This seasonality in phytoplankton growth rates and turnover times supports

the suggestion of light-limited growth in autumn and nutrient-stress in summer, as well as the rapid development of the spring bloom throughout April at CCS (Table 2; see also Mayers et al., this issue). Inefficient utilization of the P_i pool in November relative to efficient utilization in April and July is supported by the seasonal differences in turnover times of this pool; from 21.9 to 42.3 d in November to 2.7 to 8.8 d in July, with turnover times in April declining from 8.9 d to 2.2 d as the spring bloom progressed (Table 3).

Turnover of the POP pool was also slowest in November (2.8-4.9 d), with slightly faster turnover of C_{phyto} (average 1.7 d) relative to POP (average 3.9 d), which may be indicative of plankton other than phytoplankton (i.e., heterotrophic bacteria) strongly contributing to the POP pool. The relatively rapid turnover of P_i and POP during summer and late April, when P_i concentrations are depleted (<10 mmol P m^{-2}; Table 2), implies efficient P-recycling (Benitez-Nelson and Buesseler, 1999), even though these turnover times are longer than the very rapid turnover (<1 d) observed in P-limited open-ocean regions (e.g., Sohm and Capone, 2010). This efficient P-recycling in the Celtic Sea during summer supports similar levels of NPP to November, as well as relatively high rates of P_i-uptake despite the seasonal differences in P_i availability (Table 2).

Turnover times for POP in April and July were surprisingly similar (0.5-1.3 d and 1.0-1.4 d, respectively) when considering the much longer C_{phyto} turnover times in July (1.1-4.4 d; Table 3). One interpretation of this discrepancy is that the two pools were composed of different components during July, for example a greater heterotrophic bacterial contribution (or activity) in July than November or April. Estimates of euphotic zone integrated bacterial biomass (C_{bact}; Table 2) were very similar in November and July, and highest in April. However, bacterial growth efficiency, due to low respiratory C-losses and high C-fixation, were highest at CCS in July (61 ± 5%) rather than in November (27 ± 3%) or April (36 ± 6%) (Garcia-Martin et al., this issue-A). Though July C_{bact} was similar to levels seen in November (and lower than in April), its turnover time was much shorter in July; combining average values of bacterial production (see Garcia-Martin et al. (this issue-A) with average integrated bacterial biomass (Table 2) gives turnover times of 1.2 d in July, 4.7 d in November and 5.6 d in April. These C_{bact} turnover times are similar to those for the POP pool in both July and November (1.1 d and 3.9 d, respectively), but not in April (0.9 d) (Table 3). These similarities likely indicate a significant bacterial contribution to both P_i-uptake rates and the POP pool in November and July. Though C_{bact} increased relative to C_{phyto} in April (Table 2), bacterial production remained low due to low growth efficiencies (Garcia-Martin et al., this issue-A) suggesting that C_{bact} may have had less influence on Pi-uptake in April than in November or July.

The turnover times for the DOP pool were much longer (>40 d) than those for the other pools (Table 3), although much shorter turnover (<10 d) did occur during late April. Slow turnover of DOP in November was driven by relatively high DOP concentrations (11-25 mmol P m^{-2}) and moderate DOP production (0.11-0.28 mmol P m^{-2} d^{-1}), although this sampling period also had the highest overall relative percentage extracellular release (31-58%) (Table 3). July had similar slow rates of DOP turnover to November (Table 3), though lower DOP concentrations and DOP production rates (and the lowest overall extracellular release, ranging from 2-11%) (Table 2). Hence, during both November and July the DOP pool was largely refractory, with a large pool size relative to low rates of DOP production. A contrasting situation was found at CCS during April, especially during the latter half of the month as concentrations of P_i declined below ~10 mmol P m^{-2} (<200 nmol P L^{-1}) and DOP production rates increased above ~0.5 mmol P m^{-2} d^{-1} (Tables 1 and 2). Relatively short turnover times (range 4-17 d; Table 3) during the latter half of April could potentially indicate a degree of DOP utilization by the plankton community during the latter stages of the spring bloom as inorganic nutrient sources declined (and both C_{phyto} and C_{bact} increased; Table 2) and the bioavailability of DOP may have increased (see Björkman et al., 2000).

4.4. Seasonality in particulate stoichiometry in the Celtic Sea

The last two sections have highlight how seasonal variability in P_i-uptake and P-retention at CCS related to both the composition of the plankton community (C_{phyto}, C_{bact}) and resource (P_i, light) availability. In November, light-limitation caused an ecosystem composed of slow growing phytoplankton and bacteria which led to low P_i-uptake and high DOP production. In July, nutrient-stress (low P_i, NO_x) led to an efficient recycling ecosystem with slow growing phytoplankton, and fast-growing bacteria influencing both high P_i-uptake and low DOP production. The spring bloom in April was transitional between these two situations, though fast growing phytoplankton dominated P_i-uptake with increasing DOP production (and possible utilization) as inorganic nutrient resources declined (P_i, NO_x) towards the latter stages of the spring bloom. Such seasonal variability in P_i-uptake, P-release (via DOP production), plankton composition and NPP (C-fixation) will all result in variability in the stoichiometric ratio of C to P uptake.

Taking the ratio of NPP to P_i-uptake (mol:mol) as indicative of the planktonic C:P (i.e. DIC:P_i) uptake ratio shows clear seasonality (Table 3). Average ratios of NPP:P_i-uptake for each sampling period ranged from 132 (range: 75-188) in November, to 116 (54-256) in April and 44 (21-53) in July. Relative to the canconical Redfield ratio (106:1) these ratios indicate a seasonal transition from C-rich uptake in November (and late April) to strongly P-rich uptake in July (and early April) (Table 3). It is worth noting that if total P_i-uptake (tP_i = P_i-uptake + DOP production) are considered, then the relatively high percentage extracellular release during November and late April

lead to C:P ratios which are strongly P-rich relative to the canconical Redfield ratio; with cruise averages of 81 (range: 37-123) in November, 90 (46-195) in April and 42 (20-68) in July (Table 3). However, whether net or total Pi-uptake are considered, November and April are still, on average, more C-rich in their uptake rates than July, which has more P-rich uptake.

In November, NPP:P_i-uptake ratios close to (and slight higher) than the canconical Redfield ratio are associated with an ecosystem which is light-limited, with low rates of NPP and P_i-uptake, high DOP production and, though growing slowly, a strong bacterial influence on P_i-uptake rates. The spring bloom in April is associated with a transition from light-limitation to nutrient-stress as P_i concentrations decline, with short phytoplankton turnover times (i.e., fast growth rates) slowing as resource availability declines. NPP increases to a peak in mid-April and then declines slightly with nutrient concentrations, whereas P_i-uptake remains high despite the decline in concentration (Tables 1 and 2). The ratio of NPP:P_i-uptake is low (P-rich) during early April in association with rapid phytoplankton growth rates, as is expected in nutrient-replete and optimal growth conditions (Elser et al., 2000; Sterner and Elser, 2002), and then the ratio increases (C-rich) as growth slows and nutrient levels decline (Tables 2 and 3).

The low NPP:P_i-uptake ratios (P-rich) in July are not associated with rapid phytoplankton growth (Table 3), but rather with high bacterial growth rates and a stronger bacterial influence on C:P uptake (and retention). Heterotrophic bacteria are recognised as strong competitors for P_i under nutrient depleted conditions (Thingstad et al., 1993, 1996; Duhamel and Moutin, 2009). Whilst phytoplankton cellular C:P stoichiometry is near, or slightly lower, than the canconical Redfield ratio (Geider and LaRoche, 2002; Ho et al., 2003), bacterial cellular C:P ratios are significantly more P-rich (e.g., ~50; Fagerbakke et al., 1996; Sterner and Elser, 2002; Hessen et al., 2004; Duhamel and Moutin, 2009; see also Scott et al., 2012).

When considering the Continental Shelf Pump (CSP), C-overconsumption relative to nutrient utilization (N, P) is an important factor in regulating the magnitude and efficiency of the CSP. Such C-overconsumption may occur during the nutrient-impoverished summer period, when nutrient-starved phytoplankton have high cellular C:P and may excrete C-rich DOM (Toggweiler et al., 1993; Thomas et al., 2005; Bozec et al., 2006; Kuhn et al., 2010). In this context, the P-rich uptake in July may appear paradoxical, however what has not generally been considered in the CSP is the influence of non-phytoplankton C and nutrient uptake. In this study, nutrient-improvised conditions in summer are characterised by relatively slow phytoplankton growth rates and a much greater influence from heterotrophic bacteria on P-dynamics (uptake and particulate standing stocks). Conversely, early April is also associated with P-rich conditions, which are linked to rapid phytoplankton growth rates (Elser et al., 2000; Sterner and Elser, 2002) than a bacterial influence.

Given the persistence of such P-rich (relative to the canconical Redfield ratio) uptake conditions, despite strong changes in plankton composition and resource availability it appears that the dynamics of C and P_i-uptake do not strongly contribute to an efficient CSP. Rather, the stoichiometry of other biogeochemical processes, which may be more C-rich, such as the remineralisation of organic matter (Bauer et al., 2013; Burkhardt et al., 2014) and/or zooplankton ingestion/egestion (Hessen et al., 2004) may be stronger influences on the CSP by promoting and supporting C-overconsumption.

5. Conclusions

In this study, seasonal variability in P_i-uptake and DOP production at CCS relates to both the composition of the plankton community (C_{phyto}, C_{bact}) and resource (P_i, light, NO_x) availability. In November, light-limitation led to an ecosystem composed of slow growing phytoplankton and bacteria with relatively low P_i-uptake and high DOP production. In July, nutrient-stress (low P_i, depleted NO_x) led to an efficient recycling ecosystem supporting relatively high NPP with slow growing phytoplankton, and fast-growing bacteria influencing high P_i-uptake and low DOP production. The spring bloom at CCS in April was transitional between these two situations, with fast growing phytoplankton dominating P_i-uptake with increasing DOP production (in absolute and relative terms) as inorganic nutrients declined (P_i, NO_x) towards the latter stages of the bloom.

These seasonal changes in ecosystem dynamics were associated with changes in the ratio of C to P uptake, as described by the ratio of NPP to P_i-uptake in this study, with summer relatively more P-rich in terms of uptake than November or April. Such P-rich uptake was associated with a stronger influence of efficiently growing bacteria rather than phytoplankton activity, whereas P-rich uptake in early April was associated with fast phytoplankton growth in optimal growth (bloom) conditions. These results highlight the importance of the full plankton community in terms of seasonal P-dynamics and in the underlying mechanisms supporting the CSP, as well as indicating that C-overconsumption relative to nutrient uptake is unlikely to be a dominant term determining the efficiency of the CSP. Rather, the stoichiometry of heterotrophic processes (i.e. remineralisation and respiration of organic matter) needs to be further examined.

Acknowledgements

The authors would like to acknowledge the support of the captains, officers and crews of the associated Shelf Sea Biogeochemistry cruises, as well as J Sharples and M Moore who acted as the Principal Scientific Officers for the November and July. This study was supported by the UK Natural Environmental Research Council via the Shelf Sea Biogeochemistry research programme, through grants NE/K001701/1, NE/K002007/1 and NE/K002058/1. KM was supported by a NERC

Doctoral Training Partnership (DTP) studentship as part of the Southampton Partnership for Innovative Training of Future Investigators Researching the Environment (SPIFIRE).

References

Arrigo, K.R., 2005. Marine microorganisms and global nutrient cycles. Nature 437, di: 10.1038/nature04159.

Arteaga, L., Pahlow, M., Oschlies, A., 2016. Modeled Chl:C ratio and derived estimates of phytoplankton carbon biomass and its contribution to total particulate organic carbon in the global surface ocean. Global Biogeochemical Cycles, 30, doi: 10.1002/2016GB005458.

Bauer, J.E., Cai, W-J., Raymond, P.A., Bianchi, T.S., Hopkinson, C.S., Regnier, P.A.G., 2013. The changing carbon cycle of the coastal ocean. Nature Geoscience 504, 61-70.

Benitez-Nelson, C.R., 2000. The biogeochemical cycling of phosphorus in marine systems. Earth-Science Reviews 51, 109-135.

Benitez-Nelson, C.R., Buesseler, K.O., 1999. Variability in inorganic and organic phosphorus turnover rates in the coastal ocean. Nature 398, 502-505.

Bertilsson, S., Berglund, O., Karl, D.M., Chisholm, S.W., 2003. Elemental composition of marine *Prochlorococcus* and *Synechococcus*: Implications for the ecological stoichiometry of the sea. Limnology and Oceanography 48, 1721-1731.

Björkman, K.M., Karl, D.M., 1994. Bioavailability of inorganic and organic phosphorus compounds to natural assemblages of micro-organisms in Hawaiian coastal waters. Marine Ecology Progress Series 111, 265-273.

Björkman, K.M., Thomson-Bulldis, A.L., Karl, D.M., 2000. Phosphorus dynamics in the North Pacific subtropical gyre. Marine Ecology Progress Series 22, 185-198.

Björkman, K.M., Karl, D.M., 2003. Bioavailability of dissolved organic phosphorus in the euphotic zone at Station ALOHA, North Pacific Subtropical Gyre. Limnology and Oceanography 48, 1049-1057.

Bozec, Y., Thomas, H., Schiettecatte, L-S., Borges, A.V., Elkalay, K., de Baar, H.J.W., 2006. Assessment of the processes controlling seasonal variations of dissolved inorganic carbon in the North Sea. Limnology and Oceanography 51, 2746-2762.

Burkhardt, B.G., Watkins-Brandt, K.S., Defforey, D., Paytan, A., White, A.E., 2014. Remineralization of phytoplankton-derived organic matter by natural populations of heterotrophic bacteria. Marine Chemistry 163, 1-9.

Burson, A., Stomp, M., Akil, L., Brussaard, C.P.D., Huisman, J., 2016. Unbalanced reduction of nutrient loads has created an offshore gradient from phosphorus to nitrogen limitation in the North Sea. Limnology and Oceanography 61, 869-888, doi: 10.1002/lno.10257.

Davis, C.E., Mahaffey, C., Wolff, G.A., Sharples, J., 2014. A storm in a shelf sea: Variability in phosphorus distribution and organic matter stoichiometry. Geophysical Research Letters 41, doi: 10.1002/2014GL061949.

Davis, C.E., Mahaffey, C., Wolff, G.A., Sharples, J. What's the matter: Seasonal organic matter dynamics across a temperate shelf sea. Progress in Oceanography, this issue.

Donald, K.M., Joint, I., Rees, A.P., Woodward, E.M.S., Savidge, G., 2001. Uptake of carbon, nitrogen and phosphorus by phytoplankton along the 20^{o}W meridian in the NE Atlantic between 57.5^{o}N and 37^{o}N. Deep-Sea Research II 48, 873-897.

Duhamel, S., Moutin, T., 2009. Carbon and phosphate incorporation rates of microbial assemblages in contrasting environments in the Southeast Pacific. Marine Ecology Progress Series 375, 53-64.

Duhamel, S., Dyhrman, S.T., Karl, D.M., 2010. Alkaline phosphatase activity and regulation in the North Pacific Subtropical Gyre. Limnology and Oceanography 55, 1414-1425.

Duhamel, S., Björkman, K.M., Karl, D.M., 2012. Light dependence of phosphorus uptake by microorganisms in the subtropical North and South Pacific Ocean. Aquatic Microbial Ecology 67, 225-238.

Duhamel, S., Björkman, K.M., Doggett, J.K., Karl, D.M., 2014. Microbial response to enhanced phosphorus cycling in the North Pacific Subtropical Gyre. Marine Ecology Progress Series 504, 43-58.

Duhamel, S., Bjorkman, K.M., Repeta, D.J., Karl, D.M., 2017. Phosphorus dynamics in biogeochemically distinct regions of the southeast subtropical Pacific Ocean. Progress in Oceanography 151, 261-274.

Dyhrman, S.T., Ammerman, J.W., Van Mooy, B.A.S., 2007. Microbes and the marine phosphorus cycle. Oceanography 20, 110-116.

Dyhrman, S.T., Ruttenberg, K.C., 2006. Presence and regulation of alkaline phosphatase activity in eukaryotic phytoplankton from the coastal ocean: Implications for dissolved organic phosphorus remineralization. Limnology and Oceanography 51, 1381-1390.

Elser, J.J., Kyle, M., Makino, W., Yoshida, T., Urabe, J., 2003. Ecological stoichiometry in the microbial food web: a test of the light: nutrient hypothesis. Aquatic Microbial Ecology 31, 49-65.

Finkel, Z.V., Quigg, A., Raven, J.A., Reinfelder, J.R., Schofield, O.E., Falkowski, P.G., 2006. Irradiance and the elemental stoichiometry of marine phytoplankton. Limnology and Oceanography 51, 2690-2701.

García-Martín, E.E., Daniels, C.J., Davidson, K., Davis, C.E., Mahaffey, C., Mayers, K.M.J., McNeil, S., Poulton, A.J., Purdie, D.A., Tarran, G., Robinson, C. Seasonal changes in microplankton respiration and bacterial metabolism in a temperate Shelf Sea. Progress in Oceanography, this issue-A.

García-Martín, E.E., Daniels, C.J., Davidson, K., Lozano, J., Mayers, K.M.J., McNeil, S., Mitchell, E., Poulton, A.J., Purdie, D.A., Tarran, G., Whyte, C., Robinson, C. Plankton community respiration and bacterial metabolism in a North Atlantic shelf sea during spring bloom development (April 2015). Progress in Oceanography, this issue-B.

Geider, R., La Roche, J., 2002. Redfield revisited: variability of C:N:P in marine microalgae and its biochemical basis. European Journal of Phycology 37, 1-17.

Goldman, J.C., McCarthy, J.J., Peavey, D.G., 1979. Growth rate influence on the chemical composition of phytoplankton in oceanic waters. Nature 279, 210-215.

Hessen, D.O., Færøvig, P.J., Andersen, T., 2002. Light, nutrients, and P:C ratios in algae: Grazer performance related to food quality and quantity. Ecology 83, 1886-1898.

Hessen, D.O., Ågren, G.I., Anderson, T.R., Elser, J.T., de Ruiter, P.C., 2004. Carbon sequestration in ecosystems: The role of stoichiometry. Ecology 85, 1179-1192.

Hessen, D.O., Leu, E., Færøvig, P.J., Petersen, S.F., 2008. Light and spectral properties as determinants of C:N:P-ratios in phytoplankton. Deep-Sea Research II 55, 2169-2175.

Hickman, A., Poulton, A.J., Daniels, C.J., Mayers, K.M.J., Tarran, G.A. Seasonal variability in size-fractionated chlorophyll-*a* and primary production in the Celtic Sea. Progress in Oceanography, this issue.

Ho, T-Y., Quigg, A., Finkel, Z.V., Milligan, A.J., Wyman, K., Falkowski, P.G., Morel, F.M.M., 2003. The elemental composition of some marine phytoplankton. Journal of Phycology 39, 1145-1159.

Humphreys, M.P., Moore, C.M., Achterberg, E.P., Hartman, S.E., Kivimae, C., Griffiths, A.M., Smilenova, A., Chowdhury, M.Z.H., Hull, T., Woodward, E.M.S., Wihsgott, J., Hopkins, J.E. Mechanisms for a nutrient-conservative carbon pump in a seasonally stratified, temperate continental shelf sea. Progress in Oceanography, this issue.

Joint, I., Wollast, R., Chou, L., Batten, S., Elskens, M., Edwards, E., Hirst, A., Burkill, P., Groom , S., Gibb, S., Miller, A., Hydes, D., Dehairs, F., Antia, A., Barlow, R., Rees, A., Pomroy, A., Brockmann, U., Cummings, D., Lampitt, R., Loijens, M., Mantoura, F., Miller, P., Raabe, T.,

Alvarez-Salgado, X., Stelfox, C., Woolfenden, J., 2001. Pelagic production at the Celtic Sea shelf break. Deep-Sea Research Part II 48, 14-15.

Karl, D.M., 2000. Phosphorus, the staff of life. Nature 406, 31-33.

Karl, D.M., Tien, G., 1992. MAGIC: A sensitive and precise method for measuring dissolved phosphorus in aquatic environments. Limnology and Oceanography 37, 103-116.

Klausmeier, C.A., Litchman E., Daufresne, T., Levin, S.A., 2004. Optimal nitrogen-to-phosphorus stoichiometry of phytoplankton. Nature 429, 171-174.

Kovala, P.E., Larrence, J.D., 1966. Computation of phytoplankton number, cell volume, cell surface and plasma volume per litre, from microscopic counts. Special Report No. 38, Department of Oceanography, University of Washington.

Leynaert, A., Tréguer, P., Lancelot, C., Rodier, M., 2001. Silicon limitation of biogenic silica production in the Equatorial Pacific. Deep-Sea Research I 48, 639-660.

Lopez, J., Garcia, N.S., Talmy, D., Martiny, A.C., 2016. Diel variability in the elemental composition of the marine cyanobacterium *Synechococcus*. Journal of Plankton Research 38, 1052-1061.

Martiny, A.C., Talarmin, A., Mouginot, C., Lee, J.A., Huang, J.S., Gellene, A.G., Caron, D.A., 2016. Biogeochemical interactions control a temporal succession in the elemental composition of marine communities. Limnology and Oceanography 61, 531-542, doi: 10.1002/lno.10233.

Mayers, K.M.J., Poulton, A.J., Daniels, C.J, Wells, S.R., Woodward, E.M.S., Tyrrell, T., Giering, S.L.C. Top-down control of coccolithophore populations during spring in a temperate Shelf Sea (Celtic Sea, April 2015). Progress in Oceanography, this issue.

Moore, C.M., Mills, M.M., Arrigo, K.R., Berman-Frank, I., Bopp, L., Boyd, P.W., Galbraith, E.D., Geider, R.J., Guieu, C., Jaccard, S.L., Jickells, T.D., La Roche, J., Lenton, T.M., Mahowald, N.M., Maranon, E., Marinov, I., Moore, J.K., Nakatsuka, Oschlies, A., Saito, M.A., Thingstad, T.F., Tsuda, A., Ulloa, O., 2013. Nature Geoscience 6, 701-710, doi: 10.1038/ngeo1765.

Orrett, K., Karl, D.M., 1987. Dissolved organic phosphorus production in surface waters. Limnology and Oceanography 32, 383-395.

Paytan, A., McLaughlin, K., 2007. The oceanic phosphorus cycle. Chemical Reviews 107, 563-576.

Pemberton, K., Rees, A.P., Miller, P.I., Raine, R., Joint, I., 2004. The influence of water body characteristics on phytoplankton diversity and production in the Celtic Sea. Continental Shelf Research 24, 2011-2028.

Popendorf, K.J., Duhamel, S., 2015. Variable phosphorus uptake rates and allocation across microbial groups in the oligotrophic Gulf of Mexico. Environmental Microbiology 17, 3992-4006.

Poulton, A.J., Sanders, R., Holligan, P.M., Stinchcombe, M.C., Adey, T.R., Brown, L., Chamberlain, K., 2006. Phytoplankton mineralization in the tropical and subtropical Atlantic Ocean. Global Biogeochemical Cycles 20, GB4002, doi: 10.1029/2006GB002712.

Quigg, A., Finkel, Z.V., Irwin, A.J., Rosenthal, Y., Ho, T-Y., Reinfelder, J.R., Schofield, O., Morel, F.M.M., Falkowski, P.G., 2003. The evolutionary inheritance of elemental stoichiometry in marine phytoplankton. Nature 425, 291-294.

Rees, A.P., Joint, I., Donald, K.M., 1999. Early spring bloom phytoplankton-nutrient dynamics at the Celtic Sea Shelf Edge. Deep-Sea Research I 46, 483-510.

Redfield, A.C., Ketchum, B.H., Richards, F.A., 1963. The influence of organisms on the composition of seawater. In: The sea (ed. Hill, M.N.), Wiley, 26-77.

Reynolds, S., Mahaffey, C., Roussenov, V., Williams, R.G., 2014. Evidence for production and lateral transport of dissolved organic phosphorus in the eastern subtropical North Atlantic. Global Biogeochemical Cycles 28, doi: 10.1002/2013GB004801.

Scott, J.T., Cotner, J.B., LaPara, T.M., 2012. Variable stoichiometry and homeostatic regulation of bacterial biomass elemental composition. Frontiers in Microbiology 3, 1-8.

Sohm, J.A., Capone, D.G., 2010. Zonal differences in phosphorus pools, turnover and deficiency across the tropical North Atlantic Ocean. Global Biogeochemical Cycles 24, GB2008, doi: 10.1029/2008GB003414.

Sterner, R.W., Andersen, T., Elser, J.J., Hessen, D.O., Hood, J.M., McCauley, E., Urabe, J., 2008. Scale-dependent carbon: nitrogen: phosphorus seston stoichiometry in marine and freshwaters. Limnology and Oceanography 53, 1169-1180.

Tambi, H., Flaten, G.A.F., Egge, J.K., Bodtker, G., Jacobsen, T.F. Thingstad, 2009. Relationship between phosphate affinities and cell size and shape in various bacteria and phytoplankton. Aquatic Microbial Ecology Special Issue 3, 1-10.

Tarran, G.A., Heywood, J.L., Zubkov, M.V., 2006. Latitudinal changes in the standing stocks of nano- and picoeukaryotic phytoplankton in the Atlantic Ocean. Deep-Sea Research II 53, 1516-1529.

Thingstad, T.F., Skjoldal E.F., Bohne, R.A., 1993. Phosphorus cycling and algal-bacterial competition in Sandsfjord, western Norway. Marine Ecology Progress Series 99, 239-259.

Thingstad, T.F., Riemann, B., Havskum, H., Garde, K., 1996. Incorporation rates and biomass content of C and P in phytoplankton and bacteria in the Bay of Aarhus (Denmark) June 1992. Journal of Plankton Research 18, 97-121.

Thomson-Bulldis, A., Karl, D.M., 1998. Application of a novel method for phosphorus determinations in the oligotrophic North Pacific Ocean. Limnology and Oceanography 43, 1565-1577.

Urabe, J., Sterner, R.W., 1996. Regulation of herbivore growth by the balance of light and nutrients. Proceedings of the National Academy of Sciences 93, 8465-8469.

Wihsgott, J.U., Sharples, J., Hopkins, J.E., Woodward, E.M.S., Greenwood, N., Hull, T., Sivyer, D.B. Investigating the autumn bloom's significance within the seasonal cycle of primary production in a temperate shelf sea. Progress in Oceanography, this issue.

Widdicombe, C.E., Eloire, D., Harbour, D., Harris, R.P., Somerfield, P.J., 2010. Long-term phytoplankton community dynamics in the Western English Channel. Journal of Plankton Research 32, 643-655.

Yin, K., Harrison, P.J., 2016. Sequential nutrient uptake by phytoplankton maintains high primary productivity and balanced nutrient stoichiometry. Biogeosciences Discussion, doi: 10.5194/bg-2016-426.

TABLES

Table 1. Environmental characteristics at two study sites in the Celtic Sea for November (2014), April (2015) and July (2015). CCS, Central Celtic Sea study site; CS2, Shelf Edge study site; SML, surface mixed layer depth; SML Temp., average temperature of the SML; Zeup, depth of the euphotic zone; P_i, inorganic phosphate concentration; NO_x, concentration of nitrate+nitrite; N*, ratio of nitrate+nitrite to phosphate expressed after Moore et al. (2009); E_0, incidental irradiance (PAR) at the sea-surface; $\bar{E}_{SML}$, average irradiance (PAR) over the SML.

Table 2. Euphotic zone inventories of biomass, production and phosphorus dynamics at two study sites in the Celtic Sea for November (2014), April (2015) and July (2015). CCS, Central Celtic Sea study site; CS2, Shelf Edge study site; Chl-*a*, chlorophyll-*a* concentrations; C_{phyto}, phytoplankton biomass; C_{bact}, bacterial biomass; NPP, Net Primary Production; P_i, inorganic phosphate concentration; POP, particulate organic phosphate; DOP, dissolved organic phosphorus; P_i uptake, uptake of inorganic phosphate; DOP prod., production of DOP; PER, percentage extracellular release of DOP.

Table 3. Turnover times and elemental stoichiometry at two study sites in the Celtic Sea for November (2014), April (2015) and July (2015). Stoichiometry of carbon fixation (net primary production, NPP) is expressed against P_i uptake and total P_i uptake (i.e. sum of P_i uptake + DOP production) on daily timescales. CCS, Central Celtic Sea study site; CS2, Shelf Edge study site; C_{phyto}, phytoplankton carbon; P_i, inorganic phosphate; POP, particulate organic phosphate; DOP, dissolved organic phosphorus; tP_i, total P_i uptake (sum of Pi-uptake and DOP production).

SUPPLEMENTARY TABLES

Table S1. Irradiance in incubations.

Table 1.

Season / Date	Site	SML (m)	SML Temp. (^{o}C)	Zeup (m)	P_i (nmol P L^{-1})	NO_x (µmol N L^{-1})	N*	E_0 (mol PAR m^{-2} d^{-1})	$\bar{E}_{SML}$ (mol PAR m^{-2} d^{-1})
					November 2014				
10 Nov	CCS	44	13.7	40	180	2.1	-0.8	8.4	1.6
12 Nov	CCS	32	13.6	28	180	2.1	-0.8	11.9	2.3
18 Nov	CS2	58	13.9	65	280	3.5	-1.0	7.7	1.8
20 Nov	CS2	58	14.1	55	220	2.6	-1.0	9.3	1.9
22 Nov	CCS	54	13.1	43	210	1.8	-1.6	8.1	1.4
25 Nov	CCS	52	12.8	50	210	2.5	-0.9	12.1	2.5
Mean		**50**	**13.5**	**47**	**213**	**2.4**	**-1.0**	**9.6**	**1.9**
					April 2015				
04 April	CCS	51	10.0	37	491	6.1	-1.8	20.7	3.3
06 April	CCS	47	10.0	37	459	5.7	-1.7	43.2	7.4
10 April	CS2	27	11.3	48	510	8.2	0.1	18.1	6.5
11 April	CCS	22	10.3	32	330	3.8	-1.5	42.3	12.8
15 April	CCS	25	10.6	28	190	1.2	-1.9	20.0	4.8
20 April	CCS	24	10.6	28	190	2.0	-1.0	41.4	10.3
24 April	CS2	24	11.7	30	190	2.3	-0.7	45.4	12.0
25 April	CCS	16	11.1	35	130	0.4	-1.7	42.0	17.5
Mean		**30**	**10.7**	**34**	**311**	**3.7**	**-1.7**	**34.1**	**9.3**
					July 2015				
14 July	CCS	28	16.0	53	90	<0.02	-1.4	23.2	8.7
15 July	CCS	30	16.1	52	90	<0.02	-1.4	33.2	11.6
19 July	CS2	11	15.8	20	70	<0.02	-1.1	26.1	9.5
20 July	CS2	12	16.2	25	80	0.17	-1.1	49.8	20.1
24 July	CCS	22	16.8	55	80	<0.02	-1.3	26.2	12.0
29 July	CCS	35	16.2	46	60	<0.02	-0.9	41.5	11.5
30 July	CCS	43	16.3	46	55	<0.02	-0.9	49.4	11.3
Mean		**26**	**16.2**	**42**	**76**	**0.04**	**-1.2**	**35.6**	**12.1**

Table 2.

Season / Date	Site	Chl-*a*	C_{phyto}	C_{bact}	NPP	P_i	POP	DOP	P_i uptake	DOP prod.	PER	Chl-*a* normalised		
												P_i uptake	DOP prod.	NPP
		(mg m^{-2})	(mmol C m^{-2})		(mmol C m^{-2} d^{-1})	(mmol P m^{-2})			(mmol P m^{-2} d^{-1})		(%)	(nmol P (µg Chl-*a*)$^{-1}$ d^{-1})		(gC (g Chl-*a*)$^{-1}$ h^{-1})
						November 2014								
10 Nov	CCS	59.7	91	28	37.0	7.6	1.7	14	0.24	-	-	4.0	-	0.8
12 Nov	CCS	37.4	36	-	18.5	5.2	-	-	0.14	0.19	58	3.7	5.1	0.7
18 Nov	CS2	54.4	78	24	22.5	18.3	2.0	25	0.30	0.28	48	5.5	5.1	0.6
20 Nov	CS2	57.6	73	24	26.3	12.0	1.4	13	0.24	0.11	31	4.2	1.9	0.6
22 Nov	CCS	68.7	91	32	42.9	9.0	1.0	11	0.25	0.13	34	3.6	1.9	0.8
25 Nov	CCS	70.8	93	32	46.9	10.5	1.1	19	0.25	0.17	34	3.5	1.8	0.9
Mean		**58.1**	**77**	**28**	**32.4**	**10.4**	**1.4**	**16**	**0.24**	**0.17**	**41**	**4.1**	**3.2**	**0.7**
						April 2015								
04 April	CCS	49.6	153	49	117.6	18.3	1.0	12	1.43	0.11	7	28.8	2.2	2.0
06 April	CCS	61.4	162	57	59.1	17.3	-	-	1.03	0.12	10	16.8	2.0	0.8
10 April	CS2	37.8	106	27	87.8	25.1	1.1	13	1.64	0.26	14	43.4	6.9	2.0
11 April	CCS	94.9	221	142	154.0	11.1	3.1	13	1.68	0.36	18	17.7	3.8	1.4
15 April	CCS	152.6	180	162	532.1	6.7	3.1	10	2.08	0.65	24	13.6	4.3	3.0
20 April	CCS	92.3	168	182	206.2	5.3	2.4	9	1.89	0.82	30	20.5	8.9	1.9
24 April	CS2	57.4	202	44	132.8	5.7	2.1	6	1.33	1.11	45	23.2	19.3	2.0
25 April	CCS	110.4	247	142	321.0	5.7	3.5	12	1.76	0.48	21	15.9	4.3	2.5
Mean		**82.1**	**180**	**101**	**201.3**	**11.9**	**2.3**	**11**	**1.61**	**0.49**	**21**	**22.5**	**6.5**	**2.0**
						July 2015								
14 July	CCS	19.3	200	30	58.5	6.3	2.2	7	1.11	0.02	2	57.5	1.0	2.3
15 July	CCS	28.5	121	23	43.7	6.6	-	-	1.18	-	-	41.4	-	1.2
19 July	CS2	18.4	66	32	32.5	1.8	1.0	3	0.72	0.04	5	39.1	2.2	1.3
20 July	CS2	17.2	-	-	18.3	2.1	-	-	0.53	0.03	5	30.8	1.7	0.8
24 July	CCS	35.7	86	33	38.3	12.2	-	-	0.96	0.07	7	26.9	2.0	0.8
29 July	CCS	26.4	79	27	19.7	4.2	1.3	10	0.92	0.08	8	24.8	3.0	0.6
30 July	CCS	28.0	-	-	36.8	5.3	-	-	0.48	0.06	11	17.1	2.1	1.0
Mean		**24.8**	**110**	**29**	**35.4**	**5.5**	**1.5**	**7**	**0.84**	**0.05**	**6**	**35.4**	**2.0**	**1.1**

Table 3.

Season / Date	Site	C_{phyto}	P_i	POP	DOP	Daily NPP:P_i uptake	Daily NPP:tPi uptake
			[d^{-1}]				[mol C:mol P]
					November 2015		
10 Nov	CCS	1.5	21.9	4.9	-	154	-
12 Nov	CCS	1.9	25.7	-	-	132	56
18 Nov	CS2	2.2	42.3	4.6	62	75	37
20 Nov	CS2	2.0	34.7	4.0	83	110	75
22 Nov	CCS	1.5	25.0	2.8	59	172	113
25 Nov	CCS	1.4	29.1	3.0	102	188	123
Mean		**1.7**	**29.8**	**3.9**	**77**	**132**	**81**
					April 2015		
04 April	CCS	0.7	8.9	0.5	78	82	76
06 April	CCS	1.7	11.6	-	-	57	51
10 April	CS2	0.7	10.6	0.5	35	54	46
11 April	CCS	1.0	4.6	1.3	24	92	75
15 April	CCS	0.5	2.2	1.0	11	256	195
20 April	CCS	0.7	1.9	0.9	8	109	76
24 April	CS2	0.7	3.0	1.1	4	100	54
25 April	CCS	0.6	2.2	1.4	17	182	143
Mean		**0.8**	**5.6**	**0.9**	**25**	**116**	**90**
					July 2015		
14 July	CCS	1.1	3.9	1.4	239	53	52
15 July	CCS	2.1	3.9	-	-	37	-
19 July	CS2	1.9	1.7	1.0	45	45	43
20 July	CS2	3.1	2.7	-	-	35	33
24 July	CCS	3.1	8.8	-	-	40	37
29 July	CCS	4.4	3.2	1.0	88	21	20
30 July	CCS	2.5	7.7	-	-	77	68
Mean		**2.6**	**4.6**	**1.1**	**124**	**44**	**42**

FIGURES

Figure 1. Location of the sampling stations in the Celtic Sea for this study: CCS, Central Celtic Sea site; CS2, Shelf edge site.

Figure. 2. Box and whisker plots of: (a) phosphate (P_i) concentration (nmol P L^{-1}); (b) chlorophyll-*a* (Chl-*a*) concentration (mg m^{-3}); (c) dissolved organic phosphorus (DOP) concentration (nmol P L^{-1}); and (d) particulate organic phosphorus (POP) concentration (nmol P L^{-1}).

Figure 3. Box and whisker plots of: (a) phosphate (P_i) uptake (nmol P L^{-1} h^{-1}); (b) the ratio of light to dark P_i-uptake (L:D); and (c) chlorophyll-*a* normalised P_i-uptake (nmol P (µg Chl-*a*)$^{-1}$ h^{-1}).

Figure. 4. Box and whisker plots of: (a) dissolved organic phosphorus (DOP) production (nmol P L^{-1} h^{-1}); (b) the ratio of light to dark P_i-uptake (L:D); (c) chlorophyll-*a* normalised P_i-uptake (nmol P (µg Chl-*a*)$^{-1}$ h^{-1}); and (d) dissolved organic phosphorus (DOP) production expressed as a percentage of total P_i-uptake (Percentage Extracellular Release, PER).

Figure 5. Time-series measurements of P_i uptake for two temporal experiments: (a) hourly P_i-uptake rates at 4 h time points over 24 h; and (b) cumulative P_i-uptake over 24 h. Dashed vertical lines indicate sunset (21:00 GMT) and sunrise (05:00 GMT). Cumulative P_i-uptake was 17.1 nmol P L^{-1} d^{-1} and 22.7 nmol P L^{-1} d^{-1}, respectively.

Figure 6. Box and whisker plots of P_i turnover (d^{-1}) calculated following Bjorkman et al. (2000).

SUPPLEMENTARY FIGURES

S1. Size-fractionated Pi-uptake for surface waters at three sites in the Celtic Sea.

Fig. 1.

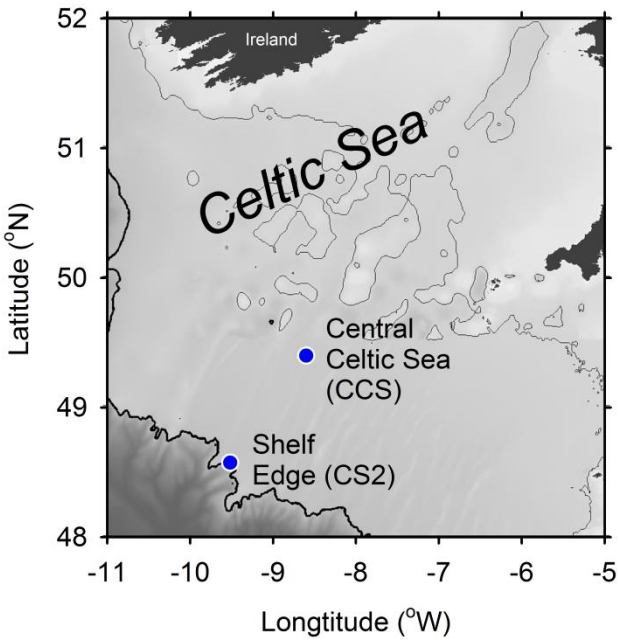
Ireland
Celtic Sea
Central
Celtic Sea
(CCS)
Shelf
Edge (CS2)
52
51
50
49
48
-11
-10
-9
-8
-7
-6
-5
Latitude (°N)
Longtitude (°W)

Fig. 2.

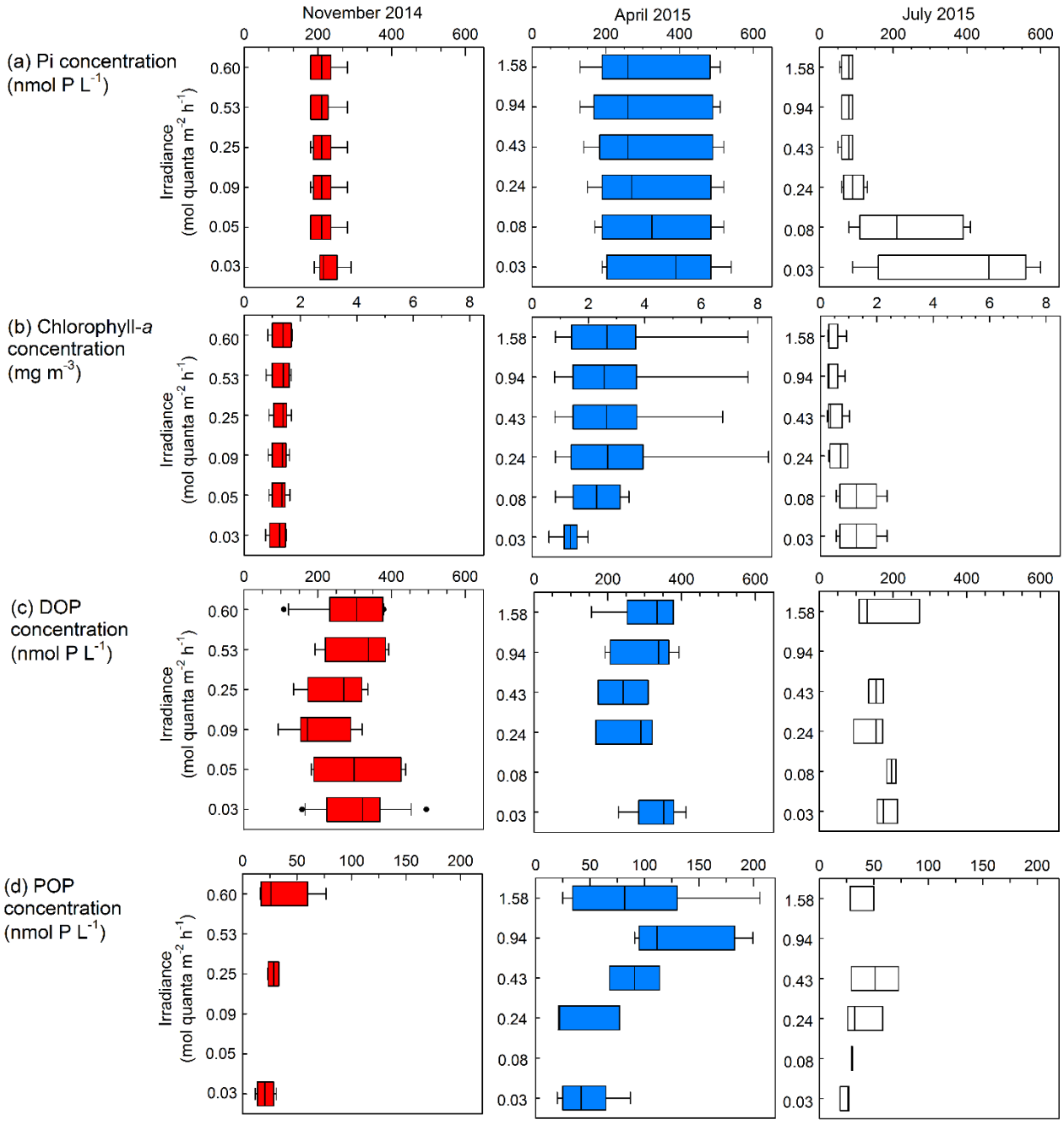
November 2014
April 2015
July 2015
(a) Pi concentration (nmol P L-1)
(b) Chlorophyll-a concentration (mg m-3)
(c) DOP concentration (nmol P L-1)
(d) POP concentration (nmol P L-1)
Irradiance (mol quanta m-2 h-1)
0.60
0.53
0.25
0.09
0.05
0.03
1.58
0.94
0.43
0.24
0.08
0.03
0
200
400
600
2
4
6
8
50
100
150
200

Fig. 3.

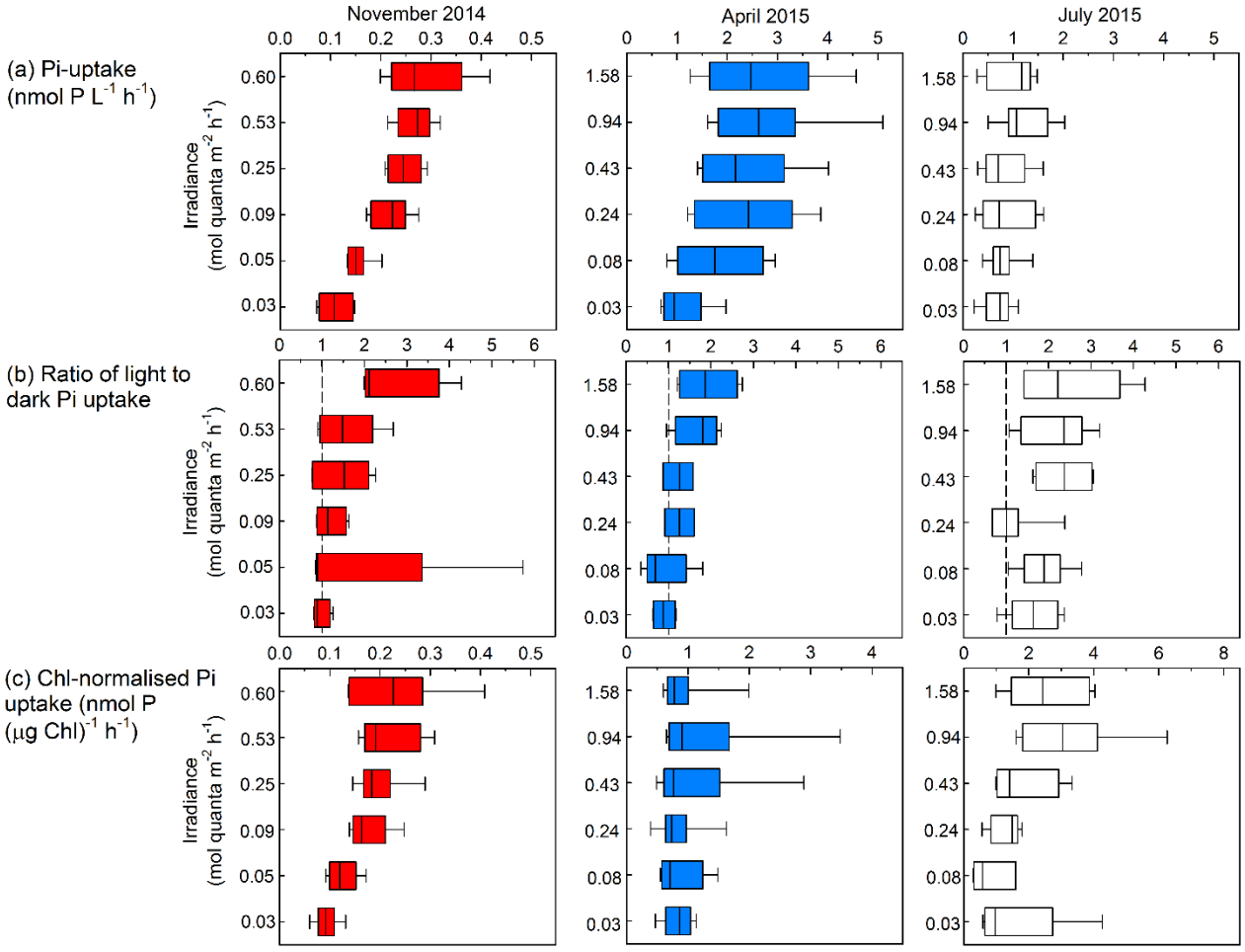
November 2014
April 2015
July 2015
(a) Pi-uptake (nmol P L-1 h-1)
(b) Ratio of light to dark Pi uptake
(c) Chl-normalised Pi uptake (nmol P (µg Chl)-1 h-1)
Irradiance (mol quanta m-2 h-1)
0.60
0.53
0.25
0.09
0.05
0.03
1.58
0.94
0.43
0.24
0.08
0.03

Fig. 4.

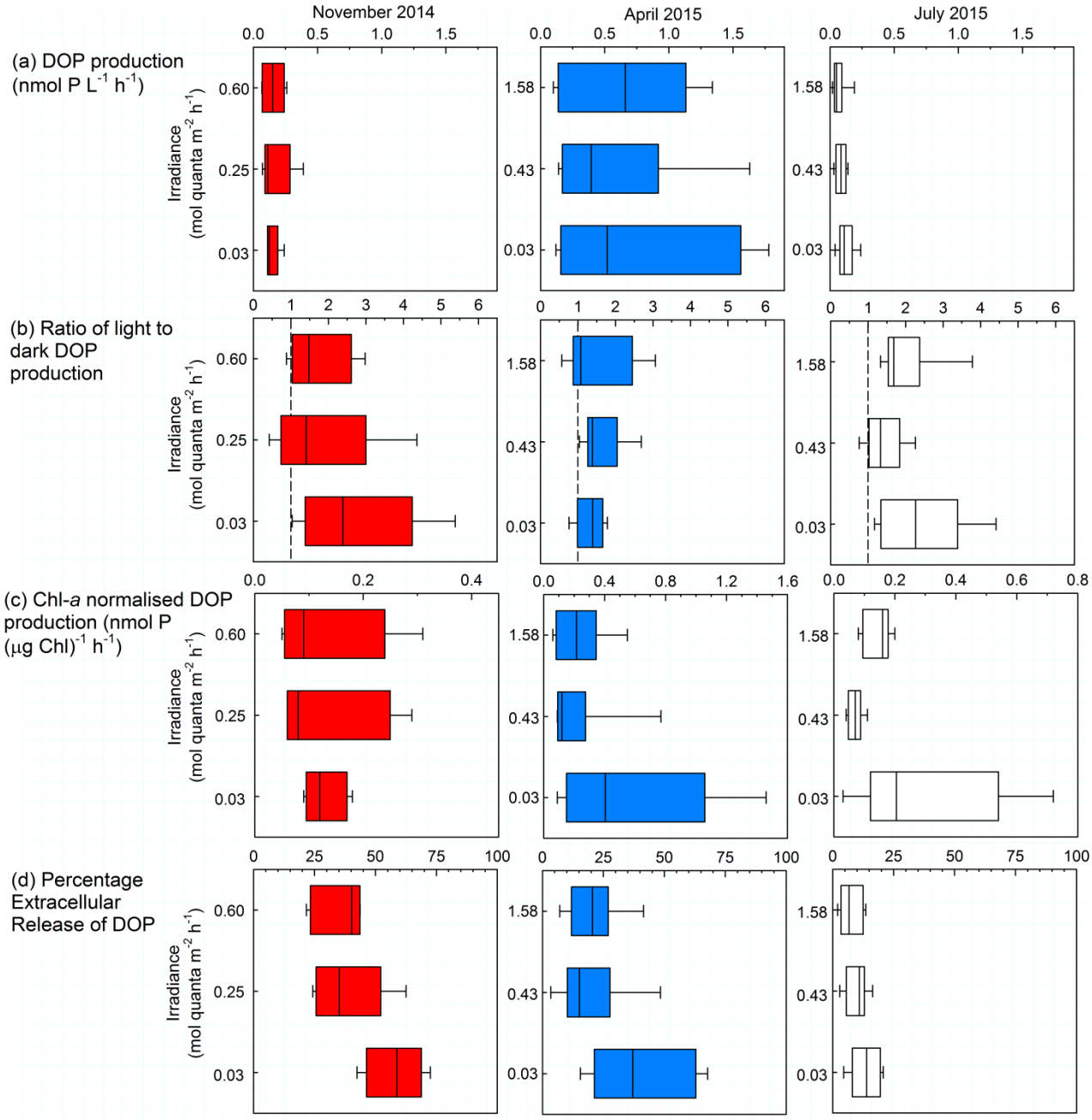
November 2014
April 2015
July 2015
(a) DOP production (nmol P L-1 h-1)
(b) Ratio of light to dark DOP production
(c) Chl-a normalised DOP production (nmol P (µg Chl)-1 h-1)
(d) Percentage Extracellular Release of DOP
Irradiance (mol quanta m-2 h-1)
0.60
0.25
0.03
1.58
0.43
0.03

Fig. 5.

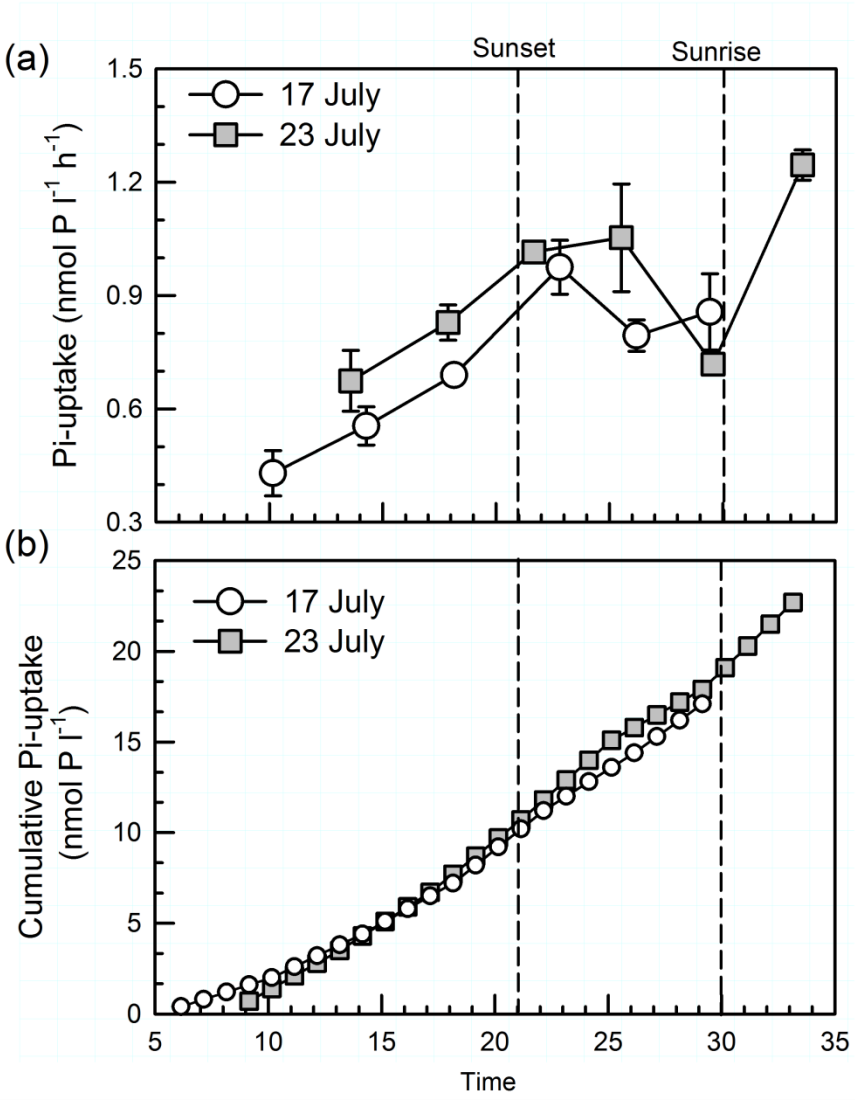
(a)
Sunset
Sunrise
17 July
23 July
Pi-uptake (nmol P l-1 h-1)
1.5
1.2
0.9
0.6
0.3
(b)
17 July
23 July
Cumulative Pi-uptake (nmol P l-1)
25
20
15
10
5
0
5
10
15
20
25
30
35
Time

Fig. 6.

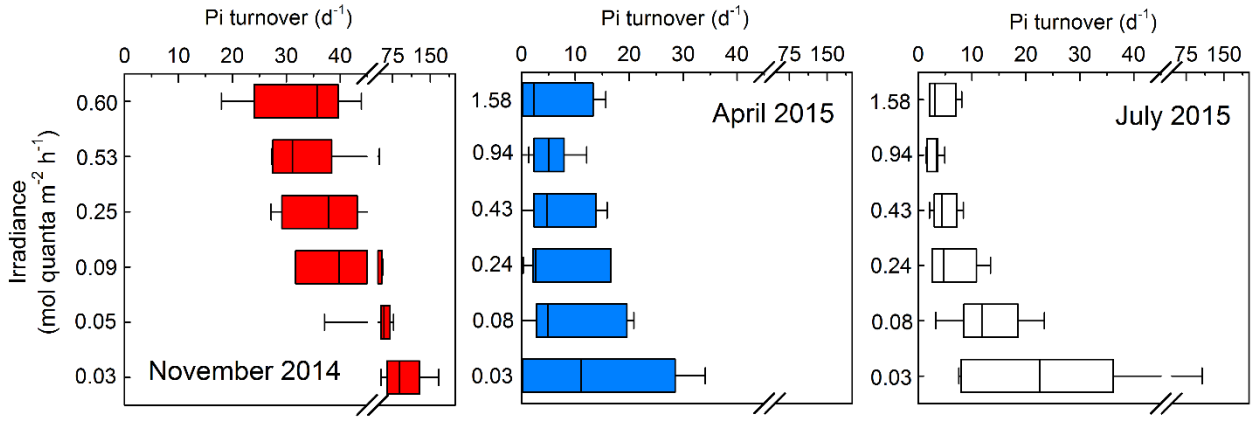
Pi turnover (d-1)
0 10 20 30 40 75 150
Irradiance (mol quanta m-2 h-1)
0.60
0.53
0.25
0.09
0.05
0.03
November 2014
Pi turnover (d-1)
0 10 20 30 40 75 150
1.58
0.94
0.43
0.24
0.08
0.03
April 2015
Pi turnover (d-1)
0 10 20 30 40 75 150
1.58
0.94
0.43
0.24
0.08
0.03
July 2015

Supplementary Table S1

Percentage Light Depth	LED Panels	Neutral density type (% transmission)	Measured Irradiance (µmol quanta m^{-2} s^{-1})	Target Photon flux (mol quanta m^{-2} d^{-1})	Actual Photon flux (mol quanta m^{-2} d^{-1})	
November 2015 (photoperiod = 9 h; E_0 = 8.7 mol quanta m^{-2} d^{-1})						
60%	2	2 x 0.15 ND (69%)	167	5.2	5.4	0.60
40%	1	None	147	3.5	4.8	0.53
20%	1	0.30 ND (51%)	70	1.7	2.3	0.25
10%	1	0.15 ND (69%)	26	0.9	0.8	0.09
5%	1	0.9 ND (14%)	15	0.4	0.5	0.05
s1%	1	1.2 ND (7%)	7	0.1	0.2	0.03
April 2015 (photoperiod = 14 h; E_0 = 33.9 mol quanta m^{-2} d^{-1})						
60%	3	None	440	20.3	22.2	1.58
40%	3	1 x 0.15 ND (69%)	260	13.5	13.1	0.94
20%	3	3 x 0.3 ND (51%)	120	6.8	6.0	0.43
10%	1	0.3 ND (51%)	68	3.4	3.4	0.24
5%	2	2 x 0.9 ND (14%)	21	1.7	1.1	0.08
1%	1	1.2 ND (7%)	7	0.3	0.4	0.03
July 2015 (photoperiod = 16 h; E_0 = 39.8 mol quanta m^{-2} d^{-1})						
60%	3	None	440	23.9	25.3	1.58
40%	3	1 x 0.15 ND (69%)	260	15.9	15.0	0.94
20%	3	3 x 0.3 ND (51%)	120	8.0	6.9	0.43
10%	1	0.3 ND (51%)	68	4.0	3.9	0.24
5%	2	2 x 0.9 ND (14%)	21	2.0	1.2	0.08
1%	1	1.2 ND (7%)	7	0.4	0.4	0.03

Supplementary Fig. S1.